AD-A141 279 SENSITIVITY ANALYSIS OF PREDICTED REACTING FLOW CHARACTERISTICS IN SOLID FUEL RAMJET COMBUSTORS(U) NAVAL POSTGRADUATE SCHOOL MONTEREY CA A S PILOS DEC 83 F/G 21/2 1/1 NL

UNCLASSIFIED

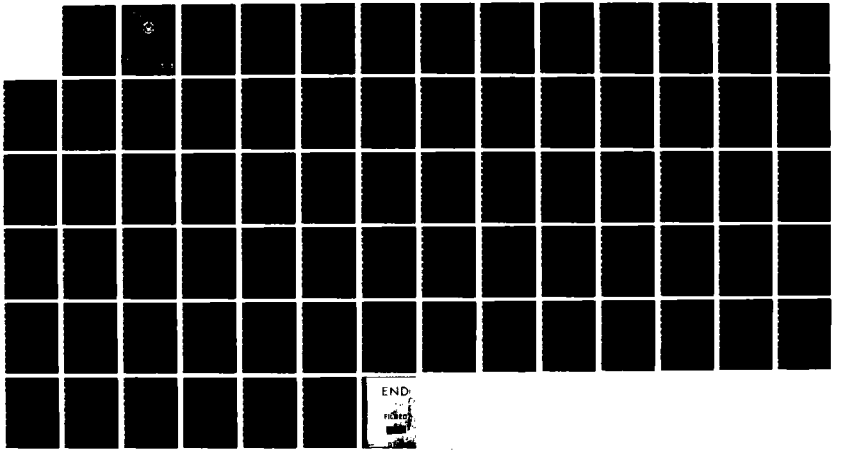

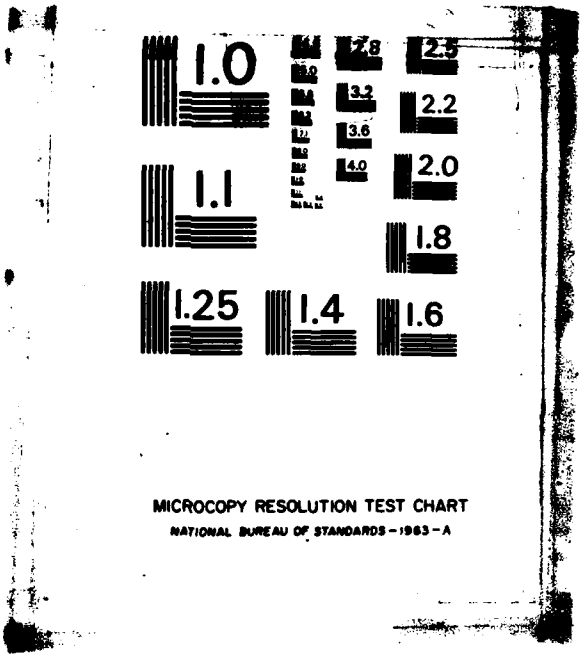
1.0
1.1
1.25
1.4
1.6
2.0
2.2
2.5
1.8
MICROCOPY RESOLUTION TEST CHART
NATIONAL BUREAU OF STANDARDS-1963-A

NAVAL POSTGRADUATE SCHOOL
Monterey, California

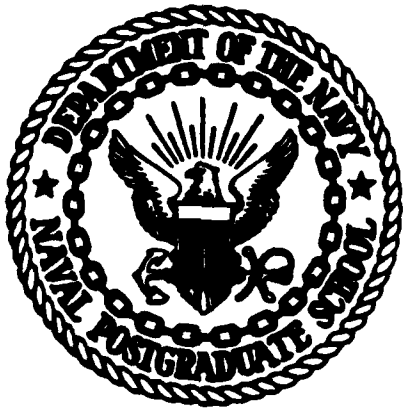

THESIS

SENSITIVITY ANALYSIS OF PREDICTED REACTING FLOW CHARACTERISTICS IN SOLID FUEL RAMJET COMBUSTORS

by

Anastasios S. Pilos

December 1983

Thesis Advisor: H.W. Burden

Approved for public release; distribution unlimited.

REPORT DOCUMENTATION PAGE		READ INSTRUCTIONS BEFORE COMPLETING FORM
1. REPORT NUMBER	2. GOVT ACCESSION NO. AD-A141279	3. RECIPIENT'S CATALOG NUMBER
4. TITLE (and Subtitle) Sensitivity Analysis of Predicted Reacting Flow Characteristics in Solid Fuel Ramjet Combustors		5. TYPE OF REPORT & PERIOD COVERED Master's Thesis; December 1983
		6. PERFORMING ORG. REPORT NUMBER
7. AUTHOR(s) Anastasios S. Pilos		8. CONTRACT OR GRANT NUMBER(s)
9. PERFORMING ORGANIZATION NAME AND ADDRESS Naval Postgraduate School Monterey, California 93943		10. PROGRAM ELEMENT, PROJECT, TASK AREA & WORK UNIT NUMBERS
11. CONTROLLING OFFICE NAME AND ADDRESS Naval Postgraduate School Monterey, California 93943		12. REPORT DATE December 1983
		13. NUMBER OF PAGES 73
14. MONITORING AGENCY NAME & ADDRESS(if different from Controlling Office)		15. SECURITY CLASS. (of this report) Unclassified
		15a. DECLASSIFICATION/DOWNGRADING SCHEDULE

16. DISTRIBUTION STATEMENT (of this Report)

Approved for public release; distribution unlimited.

17. DISTRIBUTION STATEMENT (of the abstract entered in Block 20, if different from Report)

18. SUPPLEMENTARY NOTES

19. KEY WORDS (Continue on reverse side if necessary and identify by block number)

Sensitivity Analysis
Ramjet combustors
Solid Fuel

20. ABSTRACT (Continue on reverse side if necessary and identify by block number)

This study was a sensitivity analysis of a computer code (based upon CHAMPION/2/E/FIX), used at the Naval Postgraduate School mainly to model the flow within Solid Fuel Ramjets. The purpose of the study was to make the code "simpler" and "more

#20 - ABSTRACT - (CONTINUED)

accurate by reducing the required CPUs time and/or improving the accuracy of predictions.

Accession For	
NTIS GRA&I	X
DTIC TAB	☐
Unannounced	☐
Justification	
By	
Distribution/	
Availability Codes	
Dist	Avail and/or Special
A-1	

Approved for public release; distribution unlimited.

Sensitivity Analysis of Predicted Reacting Flow Characteristics in Solid Fuel Ramjet Combustors

by

Anastasios S. Pilos
Captain, Hellenic Air Force
B.S., Naval Postgraduate School, 1982

Submitted in partial fulfillment of the requirements for the degree of

MASTER OF SCIENCE IN AERONAUTICAL ENGINEERING

from the

NAVAL POSTGRADUATE SCHOOL
December 1983

Author: A. Pilos

Approved by: _____
Thesis Advisor

_____
Chairman, Department of Aeronautics

_____
Dean of Science and Engineering

ABSTRACT

This study was a sensitivity analysis of a computer code (based upon CHAMPION/2/E/FIX), used at the Naval Post-graduate School mainly to model the flow within Solid Fuel Ramjets. The purpose of the study was to make the code "simpler" and "more accurate" by reducing the required CPUs time and/or improving the accuracy of predictions.

TABLE OF CONTENTS

LIST OF TABLES

LIST OF FIGURES

TABLE OF SYMBOLS AND ABBREVIATIONS

BP	Mass transfer number (blowing parameter)
c_1	Turbulence model empirical constant (Table I-1)
c_2	Turbulence model empirical constant (Table I-1)
c_D	Turbulence model empirical constant (Table I-1)
c_p	Specific heat at constant pressure
E	Constant, E = 9.0
f	Fuel
g	Mass transfer conductance
g*	Defined as $g^* = \lim_{BP \to 0} (g)$
h	Step height; enthalpy
$\tilde{h}$	Stagnation enthalpy
H	Dimensionless enthalpy
i	Stoichiometric coefficient
k	Turbulence kinetic energy
ℓ	Turbulence length scale
m	Mass fraction
$\dot{m}$	Mass flow rate
$\dot{m}''$	Mass flux
p	Pressure
$\dot{q}''$	Heat flux
r	Radial distance
R	Gas constant
RR,r	Regression rate

S	Source term
St	Stanton Number
T	Temperature
u	Axial velocity
v	Radial velocity
x	Axial distance from the inlet
y_p^+	Dimensionless distance of a point P from the solid boundary

GREEK SYMBOLS

γ	Ratio of specific heats
Γ	Effective transport coefficient
δ	Incremental distance from the wall
ε	Turbulence dissipation rate; emissivity
κ	Von Karman constant
μ	Viscosity
ν	Kinematic viscosity
ρ	Density
σ	Prandtl number
τ	Shear stress
ϕ	Any of the primitive variables
ϕ_c	Conserved property
χ	Defined as $\chi = m_{fu} - m_{ox}/i$
ψ	Stream function
ω	Vorticity

SUBSCRIPTS

bw	Blowing wall (fuel surface)

c	Combustion
con	Convection
eff	Effective
f	Flame
fu	Fuel
fg	Fuel grain
in	Inlet
lam	Laminar
N	Nitrogen
ox	Oxygen
p	Near-wall node
pr	Products
ref	Reference
t	Turbulent
ϕ	Referred to an independent property
w	Wall
∞	Free stream

I. INTRODUCTION

During the last fifteen years, there have been many advancements in the development of highly effective tactical weapons for use at intermediate range and with high average flight speed. One of the simplest engines/motors for such use is the Solid Fuel Ram Jet (SFRJ).

The SFRJ most often consists of a solid fuel grain which provides the walls for the combustion grain [Ref. 1]. A sudden expansion at the air inlet of the combustor can be used to provide flame stabilization by inducing recirculation into the air flow (Fig. 1.1). Combustion can be sustained throughout the grain provided that the step height (h) is sufficiently large. However, the larger the step height, the larger the losses of the inlet stagnation pressure.

Due to the sudden expansion, at least two distinct flow fields are generated within the fuel grain (Fig. 1.2). In the first field, the recirculation zone, the flow is highly turbulent and usually fuel rich. This hot gas region provides the energy necessary to sustain the combustion process which must occur further downstream. Downstream of the flow reattachment, a turbulent boundary layer develops and the combustion is diffusion controlled. A diffusion flame emanates from the recirculation zone and remains within the developing turbulent boundary layer between the

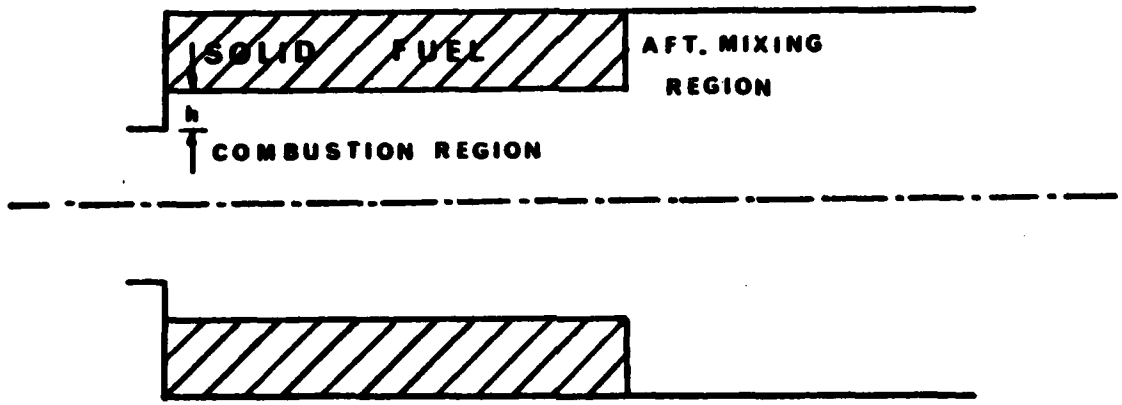

Figure 1.1. Schematic Diagram of Solid Fuel Ramjet

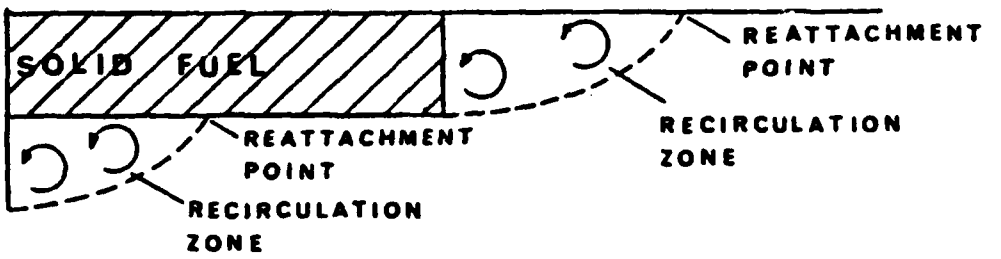

Figure 1.2. Effects of Sudden Enlargements on a SFRJ

fuel-rich zone near the wall and the oxygen-rich zone near the central core.

There have been continuing research efforts concerning the behavior of the SFRJ at the Naval Postgraduate School. Both mathematical and experimental efforts have taken place to determine the effects of design as well as operational variables of the system to be obtained.

II. DESCRIPTION OF THE COMPUTER MODEL

A. INTRODUCTION

At the NPS there have been two basic computer codes used to model the flow within solid fuel ramjets. The first one was based on stream function (ψ) and vorticity (ω) [Ref. 3]. It predicted with reasonable accuracy the velocity and temperature distributions but did not predict pressure distributions accurately and was not easily extended to complex geometries or to three-dimensional flows. The second computer model is based on the "primitive" variables, pressure (p) and velocities (u,v) [Ref. 2]. It has also been used to predict the effects of fuel properties on the SFRJ performance and to evaluate the effects of different geometries as well as operating conditions.

B. OVERVIEW OF THE PRIMITIVE VARIABLE PROGRAM

1. Assumptions

The CHAMPION/2/E/FIX computer program developed by Pun and Spalding [Ref. 2] has been used as the basis for the primitive variable model. The flow has been assumed to be steady (solid fuel grain dissipation is negligible), subsonic, recirculating, axisymmetric and to have constant specific heats. In order to calculate the effective viscosity, a modified Jones-Launder [Ref. 4] two-parameter turbulence

model has been used. It uses five empirical constants (Table II) and requires that two additional variables (turbulent kinetic energy (k) and turbulence dissipation rate (ε)) be evaluated. The effective viscosity was calculated using the formulas

$$\mu_{eff} = \mu_{lam} + \mu_t \tag{2.1}$$

where

$$\mu_t = C_D \rho \kappa^2/\varepsilon \tag{2.2}$$

TABLE I

k-ε Turbulence Model Empirical Constants

C_1	C_2	C_D	$\sigma_{k,eff}$	$\sigma_{\varepsilon,eff}$
1.43	1.92	.09	1.0	1.3

The combustion was considered to be mixing-limited (infinitely fast kinetics) with a simple one-step chemical reaction of the form:

$$1 \text{ Kg fuel} + i \text{ Kg oxidizer} \rightarrow (1+i) \text{kg products} \tag{2.3}$$

Four species were concerned: oxygen, nitrogen, fuel and products. Because of the infinitely fast kinetics

TABLE II

Governing Equation Parameters

ϕ	Γ_ϕ	S_ϕ
u	μ_{eff}	$\frac{\partial p}{\partial x}+\frac{2}{3}\frac{\partial}{\partial x}\left\{\mu\left[\frac{\partial}{\partial x}(ru)+\frac{\partial}{\partial r}(rv)\right]\right\}-\frac{\partial}{\partial x}\left(\mu\frac{\partial u}{\partial x}\right)-\frac{1}{r}\frac{\partial}{\partial r}\left(\mu r\frac{\partial v}{\partial r}\right)$
v	μ_{eff}	$\frac{\partial p}{\partial r}+2\frac{\mu v}{r^2}+\frac{2}{3}\frac{\partial}{\partial r}\left\{\frac{\mu}{r}\left[\frac{\partial}{\partial x}(\rho u)+\frac{\partial}{\partial r}(rv)\right]\right\}-\frac{\partial}{\partial x}\left(\mu\frac{\partial u}{\partial r}\right)-\frac{1}{r}\frac{\partial}{\partial r}\left(\mu r\frac{\partial v}{\partial r}\right)$
ε	$\frac{\mu_{eff}}{\sigma_\varepsilon}$	$-\frac{c_1\varepsilon}{k}\left\{\mu_t\left[2\left[\left(\frac{\partial u}{\partial x}\right)^2+\left(\frac{\partial v}{\partial r}\right)^2+\left(\frac{v}{r}\right)^2\right]+\left(\frac{\partial u}{\partial r}+\frac{\partial v}{\partial x}\right)^2\right]\right\}+\frac{c_2\rho\varepsilon^2}{k}$
k	$\frac{\mu_{eff}}{\sigma_k}$	$\rho\varepsilon-\mu_t\left\{2\left[\left(\frac{\partial u}{\partial x}\right)^2+\left(\frac{\partial v}{\partial r}\right)^2+\left(\frac{v}{r}\right)^2\right]+\left(\frac{\partial u}{\partial r}+\frac{\partial v}{\partial x}\right)^2$
$\tilde{h}$	$\frac{\mu_{eff}}{\sigma_h}$	0
$m_{fu}-\frac{m_{oa}}{i}$	$\frac{\mu_{eff}}{\sigma_j}$	0
m_{N_2}	$\frac{\mu_{eff}}{\sigma_j}$	0

$c_1 = 1.43$, $c_2 = 1.92$, $\sigma_j = \sigma_k = \sigma_h = 1$, $\sigma_\varepsilon = 1.3$

assumed, no oxygen could exist at the fuel surface and at the surface was assumed to be isothermal. The turbulent Prandtl and Schmidt numbers were taken to be equal to unity and therefore the turbulent Lewis number and laminar Prandtl number were also taken to be equal to unity.

C. GOVERNING EQUATIONS

With the above assumptions, the governing equations for axisymmetrical flows can be written as follows:

$$\frac{\partial}{\partial x}(\rho u\phi) + \frac{1}{r}\frac{\partial}{\partial r}(\rho r v\phi) - \frac{\partial}{\partial x}(\Gamma_\phi \frac{\partial \phi}{\partial x}) - \frac{1}{r}\frac{\partial}{\partial r}(r\Gamma_\phi \frac{\partial \phi}{\partial r}) + S_\phi = 0 \quad (2.4)$$

where ϕ stands for the independent variables u, v, k, ε, $\tilde{h}$, $m_{fu} - m_{ox}/i$ and m_{N_2}. The first two terms are the "convection terms", the next two the "diffusion terms". Γ_ϕ is the effective exchange coefficient for turbulent flow (Table I) and S_ϕ is the "source term" (Table II). The stagnation enthalpy for unity Prandtl and Schmidt numbers is

$$\tilde{h} = h + (u^2+v^2)/2 + \kappa \quad (2.5)$$

where for nonreacting flows

$$h \equiv c_p T \quad (2.6)$$

and for reacting flows

$$h \equiv m_{ox} \frac{\Delta H}{I} + c_p(T - T_{ref}) \tag{2.7}$$

Temperature has been calculated using Eqs. (2.5) and (2.7). Density has been calculated using the perfect gas law

$$\rho = \frac{p}{RT} \tag{2.8}$$

Since the quantities $\tilde{h}$ (stagnation enthalpy), m_{N_2} and $\chi = m_{fu} - m_{ox}/i$

have identical governing differential equations and, in appropriate dimensionless form, identical boundary conditions, a representative equation had to be solved only once. The dimensionless enthalpy was selected to be

$$H = \frac{\tilde{h}_{in} - \tilde{h}}{\tilde{h}_{in} - \tilde{h}_{fg}} \tag{2.9}$$

where $\tilde{h}_{fg}$ is the stagnation enthalpy deep in the fuel grain and $\tilde{h}_{in}$ is the stagnation enthalpy of the air at the inlet dump plane. The corresponding dimensionless forms for the other quantities were:

$$\bar{m}_{N_2} = \frac{m_{N_{2in}} - m_{N_2}}{m_{N_{2in}} - m_{N_{2fg}}} \tag{2.10}$$

and

$$x = \frac{x - x_{in}}{x_{fg} - x_{in}} \tag{2.11}$$

$$m_{fu} = x \qquad m_{ox} = 0 \qquad \text{for} \quad x \geq 0$$

$$m_{fu} = 0 \qquad m_{ox} = -x_i \qquad \text{for} \quad x < 0 \tag{2.12}$$

1. Boundary Conditions and Solution Procedure

Fixed boundary conditions (inlet velocity profile, et al.) were specified at the desired or experimentally determined values. Specified gradient boundary conditions were handled by setting the appropriate convection/diffusion coefficients to zero in the finite difference equation ("breaking the link") and then entering the appropriate gradient through linearized "false" source terms. The geometry as well as the appropriate boundary conditions are summarized in Figure (2.1).

"Plug flow" was assumed at the air inlet, although this was not a computer program limitation. The turbulence kinetic energy was assumed to be uniform, with a value which corresponded to the approximate turbulence intensity of the inlet flow. Radial and axial gradients were set equal to zero on the centerline and at the exit, respectively. All the nonreacting solid boundaries were considered adiabatic with both u and v velocity components equal to zero (no-slip condition).

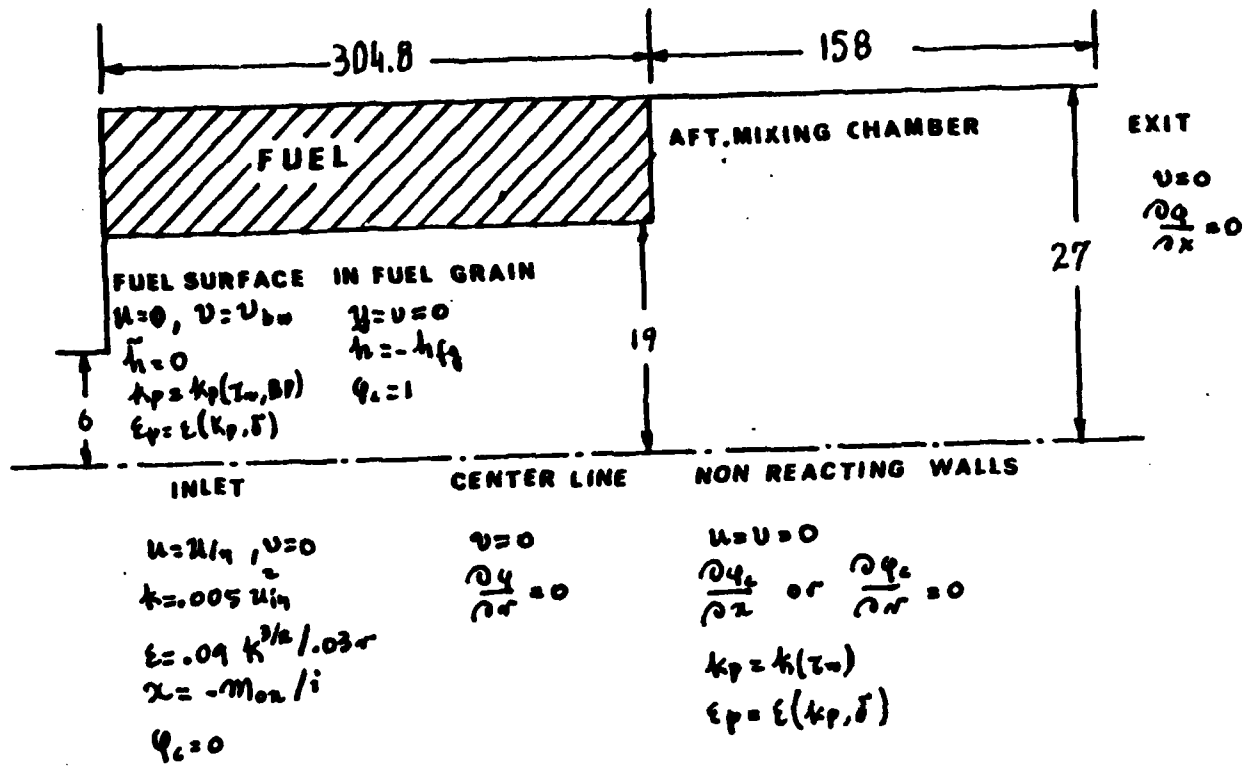

Figure 2.1. Geometry of Boundary Conditions for the SFRJ

For simplicity, the boundary layer was assumed to be composed of a laminar sublayer which is then developed to turbulent without assuming a "buffer zone". For the laminar sublayer,

$$u_p^+ = y_p^+ \tag{2.13}$$

where

$$u_p^+ \equiv \frac{u_p}{\sqrt{\tau_w/\rho}} \quad \text{and} \quad y_p^+ \equiv \frac{\sqrt{\tau_w/\rho}\, y_p}{\nu}$$

and for the rest of the layer

$$u_p^+ = \frac{\ell n (E y_p^+)}{\kappa} \tag{2.14}$$

For $E = 9.0$ and $\kappa = 0.4$ (values found from experimental data)

$$u_p^+ = 5.5 + 2.5 \ell n\, y_p^+ \tag{2.15}$$

Solving the above two equations, it is found that transition from laminar to turbulent flow occurs at $y^+ = 11.5$. The value of y_p^+ at each near-wall node is found from the relation:

$$y_p^+ = \frac{\rho \delta}{\mu_{lam}} \left(\frac{\tau_w}{\rho}\right)^{1/2} \tag{2.16}$$

For $y_p^+ < 11.5$

$$\tau_w = \frac{\mu_{lam} \cdot u_p}{\delta} \tag{2.17}$$

and for $y_p^+ > 11.5$

$$\tau_w = c_D^{1/2} \rho \kappa_p \tag{2.18}$$

The value of τ_w was assumed to be uniform from the wall to the near-wall grid point. So,

$$y_p^+ = c_D^{1/4} \rho \kappa_p^{1/2} \frac{\delta}{\mu_{lam}} \tag{2.19}$$

Then, the shear stress is calculated using the formula [Ref. 3]

$$\tau_w = c_D^{1/2} \rho \kappa_p = \rho c_D^{1/4} \kappa_p^{1/2} \left(\frac{u_p}{u_p^+}\right)$$

$$= \kappa \rho u_p \kappa_p^{1/2} \ln\left(\frac{E \rho c_D^{1/4} \kappa_p^{1/2}}{\mu_{lam}}\right) \tag{2.20}$$

where, as noted previously,

$$u_p^+ = \frac{\ln(Ey_p^+)}{\kappa}$$

Due to the steep gradients of the properties in turbulent flows near the solid boundaries, the source terms for κ and ε at the near-wall nodes were expressed in terms

of the wall shear stress. Also, τ_w provides the boundary condition for the u and v equations.

The turbulence dissipation rate ε_p at a near-wall node p is given by the relation [Ref. 3]

$$\varepsilon_p = c_D^{3/4} \kappa_p^{3/4}/\kappa\delta = \kappa_p^{3/2}/2.43\delta \qquad (2.21)$$

where the length scale is presumed to be proportional to the incremental distance from the wall,

$$\ell = c_D^{1/4} \kappa \delta \qquad (2.22)$$

It was found that when using a sudden expansion geometry in reacting flows the near-wall dissipation rate had to be increased on the step face ($\varepsilon_p = \kappa_p^{3/2}/0.4\delta$) and the grid spacing adjacent to the grain had to be fine ($y_p^+ < 11.5$) in order to obtain a temperature distribution in qualitative and quantitative agreement with experimental data [Ref. 1]. Equation (2.17) implies that the wall shear stress is calculated assuming a linear velocity profile when $y^+ < 11.5$. Therefore, a near-wall grid point can lie within the laminar sublayer but the source terms for κ and ε imply that μ_{eff}/μ_{lam} is much greater than unity. This precludes y_p^+ from being significantly less than 11.5.

For reacting flows, the boundary conditions for the dimensionless properties (Eqs. (2.9) through (2.12)) were zero

at the inlet and unity "deep" in the fuel grain. These properties were considered to have zero gradients on non-reacting surfaces.

The assumptions made for reacting flows (unity Prandtl and Schmidt numbers, simple chemical reaction, constant specific heat and stagnation enthalpy defined in Eq. (2.5)) result in a general boundary condition for all "conserved" properties (ϕ_c) on a surface which has mass transfer given by the relation [Ref. 2]

$$\dot{m}''_{bw} = (\Gamma_\phi \frac{\partial \phi_c}{\partial r})_{bw} / (\phi_{c,bw} - \phi_{c,fg}) \qquad (2.23)$$

where ϕ_c may represent h, m_{N_2} or $x = m_{fu} - m_{ox}/i$.

A mass transfer conductance (g) is often defined from the relation

$$(\Gamma_\phi \frac{\partial \phi_c}{\partial r})_{bw} = g(\phi_{c,\infty} - \phi_{c,bw}) \qquad (2.24)$$

where ϕ_∞ is defined as the free-stream value of the property.

Substituting Eq. (2.24) in Eq. (2.23), the mass transfer from the blowing wall is

$$\dot{m}''_{bw} = g(\phi_{cp} - \phi_{cbw}) / (\phi_{c,bw} - \phi_{c,fg}) \qquad (2.25)$$

where

$$BP = \frac{\phi_{cp} - \phi_{c,bw}}{\phi_{c,bw} - \phi_{c,fg}} \tag{2.26}$$

represents the mass transfer parameter (or blowing parameter). The value of g can be approximated using

$$g = (\rho u)_p \, St \tag{2.27}$$

From Reynolds' analogy with unity Prandtl number, the Stanton number is

$$ST = \frac{c_f}{2} = \frac{\tau_w}{(\rho u^2)_p} \tag{2.28}$$

where c_f is the local friction coefficient. Thus,

$$g = \frac{\tau_w}{u_p} \tag{2.29}$$

Using the Couette flow approximation for the boundary-layer behavior with mass transfer,

$$g = g^* \, \ell n(1 + BP)/BP \tag{2.30}$$

where

$$g^* = \lim_{BP \to 0} (g) \tag{2.31}$$

In this case, BP has been evaluated from the solution of the energy equation using

$$BP = \frac{\tilde{h}_{\rho} - \tilde{h}_{bw}}{\tilde{h}_{bw} - \tilde{h}_{fg}} \tag{2.32}$$

The wall shear stress has been evaluated using Eq. (2.17) or Eq. (2.20) and modified with Eq. (2.30)

$$\tau_{bw} = \tau_{w} \, \ell n(1 + BP)/BP \tag{2.33}$$

where τ_w is the wall shear stress without wall mass addition.

The mass transfer conductance (g) was evaluated using Eq. (2.29). The wall heat flux ($\dot{q}''$) on all solid isothermal boundaries was evaluated using Reynolds' analogy

$$-\dot{q}''_w/(\tilde{h}_p - \tilde{h}_w) = \frac{\tau_w}{u_p} \tag{2.34}$$

Since the blowing rates were small for the solid fuel ramjet (typically BP < 2.0), κ and ε were evaluated using Eq. (2.4) and the terms presented in Table II, which incorporate the empirical constants of Table I.

Five variables, namely u, v, κ, ε and H (or) $\tilde{h}$ were solved using Eq. (2.4) in finite difference form. The line-by-line iterative procedure employed upwind differencing and underrelaxation in order to promote convergence. On each radial line, the mass flow rate was calculated using the

local density. The "error" in mass flow (compared with the summation of "mass-in" at the upstream boundaries) was used to uniformly adjust the axial velocity over the entire line. Then, the pressure at all downstream locations was adjusted to approximately correct for the momentum imbalance created by the uniform axial velocity and a "pressure correction" equation was solved for each cell on the line. Finally, local cell velocity (axial and radial) and pressure were adjusted to satisfy cell-wise continuity.

III. ANALYSIS

A. INTRODUCTION

As previously discussed, the purpose of this study was two-fold; first, to reduce the CPU time required to run the program, without considerably affecting the accuracy of results and second, to make the program output better fit the experimental measurements without considerably increasing the CPU time. The methods used in this optimization procedure were the following:

a. Monitor the effects of the number of traverses in the tridiagonal matrix (TDMA).

b. Monitor the effects of the number of iterations.

c. Monitor the effects of the grid spacing close to the solid fuel grain wall, without changing the number of grid lines, in either the x or the r directions (constant number of nodes).

d. Monitor the effects of changes in the number of grid lines in both the x and r directions (the number of nodes was changed).

B. EFFECT OF TDMA TRAVERSES

The number of TDMA traverses in the main program is denoted by the parameter NTDMA. If there is a predominant direction of flow, this is arranged to be in the x-direction. Then, TDMA traverses are made on constant x lines, in order to make

the adjustments necessary. Generally, the greater the number of TDMA traverses, the better the accuracy obtained but the more CPU time is consumed.

C. EFFECT OF NUMBER OF ITERATIONS

The number of iterations in the main program is denoted by the parameter LSWEEP. A high number of iterations (or sweeps) is needed in order to have small residual values in the variables used. Here again the same difficulties as with the number of TDMA traverses appeared. The larger the value of LSWEEP, the better the accuracy but the greater the CPU time required. It is expected that for a high number of iterations, the increase in accuracy will be small whereas the CPU time will be excessive.

D. EFFECT OF GRID SPACING CLOSE TO THE SOLID FUEL GRAIN WALL

In the original program, the grid lines spacing close to the physical boundaries was small. For small grid spacing close to the solid fuel grain wall, the non-dimensional length y_p^+ at near wall grid points was much less than 11.5 and the flow was assumed to be laminar. The velocity profile in this case is linear, given by

$$u_p = \frac{\tau_w}{\mu_{lam}} \delta \qquad (3.1)$$

For dense packing of grid lines, the flow may be considered as laminar for more than the first node close to the

wall. In this case, the velocity profile will consist of several straight lines before turbulence will be encountered, as shown on Fig. (3.1). This could result in inaccurate predictions. The spacing was changed such that the first constant-r grid line was spaced far enough from the wall in order to have $y_p^+ > 11.5$. In this case, the velocity profile will be a logarithmic curve. If this increased spacing resulted in good predictions, then the number of constant-r grid lines could be reduced, thus reducing the total CPU time.

E. EFFECT OF CHANGES IN THE NUMBER OF GRID LINES

Generally, the greater the number of grid lines in both r and x-directions, the better the accuracy expected but also the greater the storage as well as the CPU time required to execute the program. Since it is desirable (but not necessary) to have a maximum ratio of 1.5 for distances between adjacent grid lines in the same direction and a maximum length to width ratio of 10.0 for any cell, it is preferable that both the number of constant-x and constant-r grid lines be changed (denoted by NX and NY respectively in the main program). In such a case, if the grid spacing close to the solid fuel grain wall could be increased--as discussed above--the number of lines in both directions could be reduced without affecting the accuracy of predictions. This would result in reduced requirements for storage and CPU time.

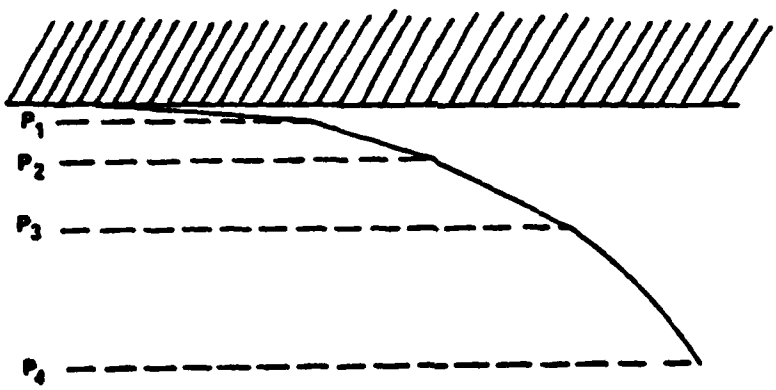

Figure 3.1. Velocity Profile Close to Solid Fuel Grain Wall

IV. RESULTS

A. INTRODUCTION

All the options discussed in the previous chapter have been tried in the modified CHAMPION/2/E/FIX computer program. The original program had been modified in the past at the Naval Postgraduate School to account for an aft-mixing chamber [Ref. 2], and for compressibility and radiation effects [Ref. 6]. This program calculates the flow in a SFRJ, whose dimensions are shown on Fig. (2.1). The input values used in the program are shown in Appendix B, which is a copy of the BLOCK DATA subroutine.

The results of interest are plotted and discussed in the following sections of this chapter. The plots mainly refer to two x-constant grid lines after the first and second sudden enlargements at x = 202 mm and x = 312 mm, respectively.

B. EFFECT OF NUMBER OF TRAVERSES

The original program has been modified to run with three different values of TDMA traverses: NTDMA = 3, NTDMA = 5 (originally used value) and NTDMA = 7. Nothing else had been changed. An attempt to run the program with NTDMA greater than 7 resulted in a repeated series of overflows after a relatively high number of iterations had taken place (LSWEEP > 20) and the program execution was terminated.

1. Temperature Distribution

The temperature profile variations were negligible in this case, as shown on Figs. (4.1) and (4.2). Thus, by using a smaller number of traverses, the accuracy of temperature distribution prediction was not significantly affected.

2. Effective Viscosity Distribution

Here again, the effect of variations of effective viscosity, as shown on Figs. (4.3) and (4.4), were negligible.

3. Axial Velocity Distribution

The axial velocity distribution after the first and second sudden enlargements are shown in Figs. (4.5) and (4.6), respectively. Once more, the number of TDMA traverses did not affect the accuracy.

C. EFFECT OF NUMBER OF ITERATIONS

The program was run for three different numbers of iterations; for LSWEEP = 100, LSWEEP = 200 (original value) and LSWEEP = 400, without any other changes.

1. y_p^+ Distribution

The values of y_p^+ after the first sudden enlargement were essentially unchanged. Some differences appeared after the second sudden enlargement but these results did not seem to depend upon the number of iterations; the peak value of y_p^+ for LSWEEP = 100 was between the peak values for LSWEEP = 200 and LSWEEP = 400. In any case, the value of y_p^+ defies accurate prediction because of recirculating flow; the relatively high value of y_p^+ was an indication of high turbulence. Thus,

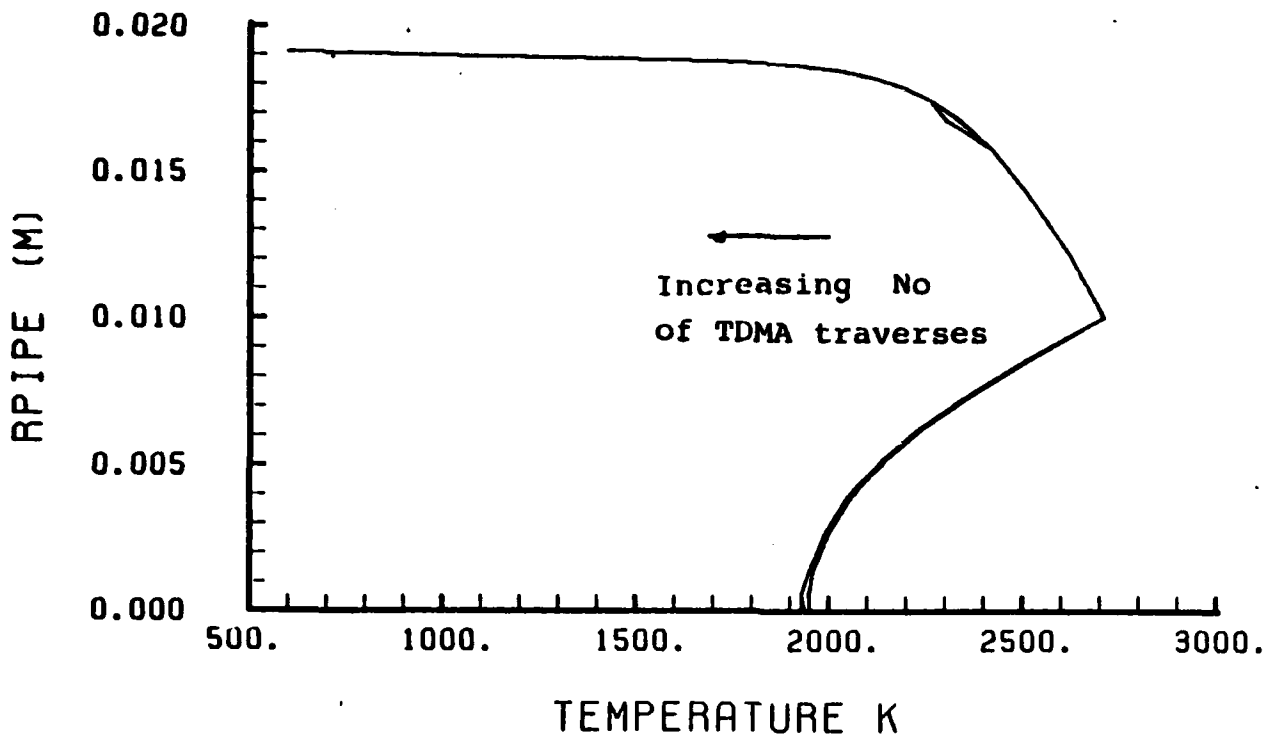

Figure 4.1. Temperature Distribution After the First Sudden Enlargement, Changing the Number of TDMA Traverses

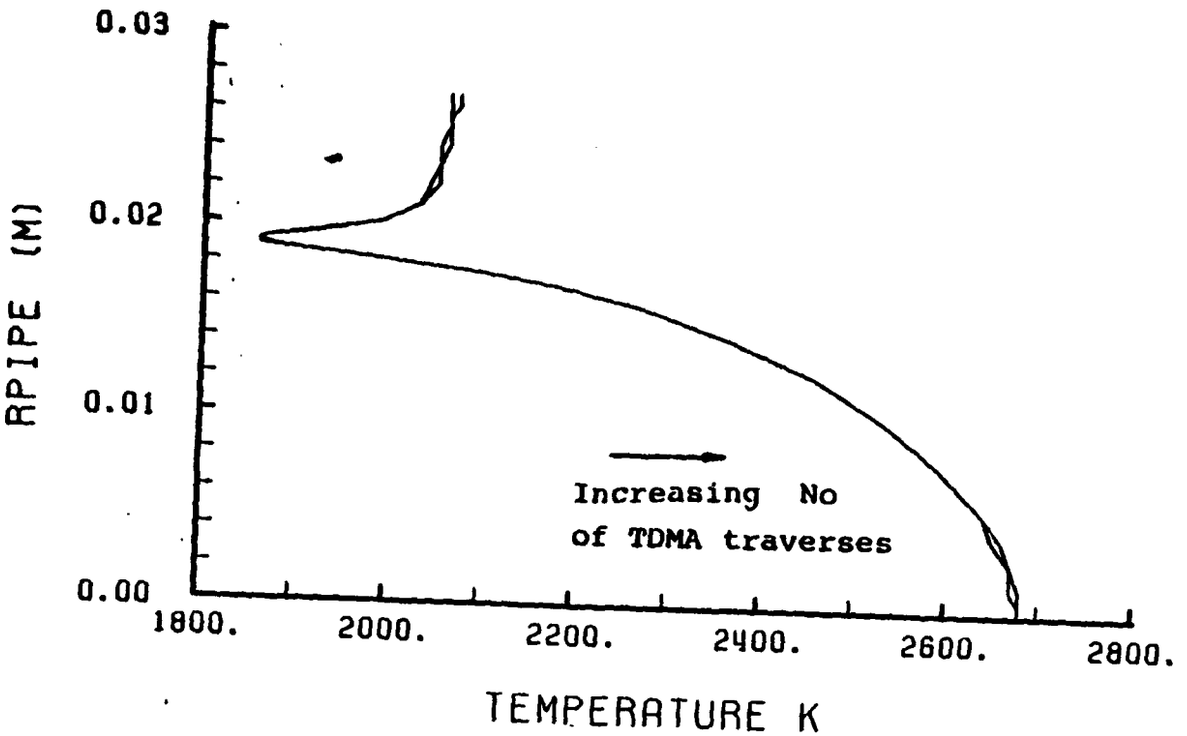

Figure 4.2. Temperature Distribution After the Second Sudden Enlargement, Changing the Number of TDMA Traverses

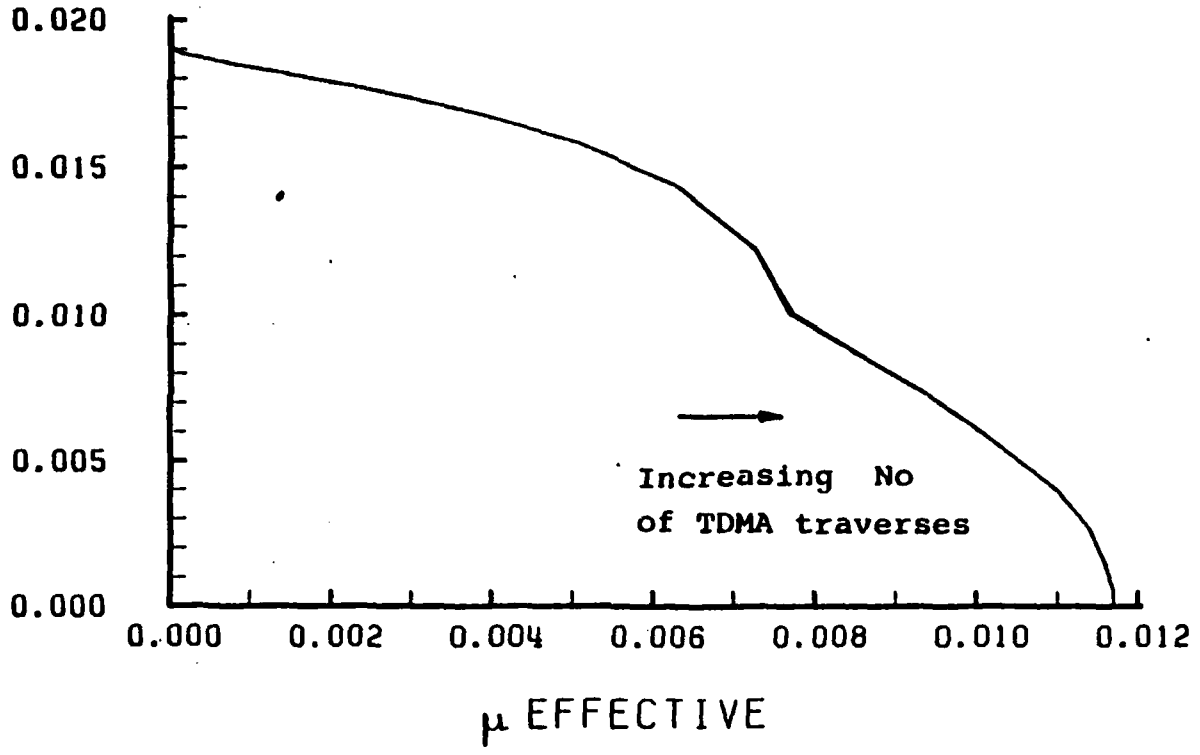

Figure 4.3. Effective Viscosity Distribution After the First Sudden Enlargement, Changing the Number of TDMA Traverses

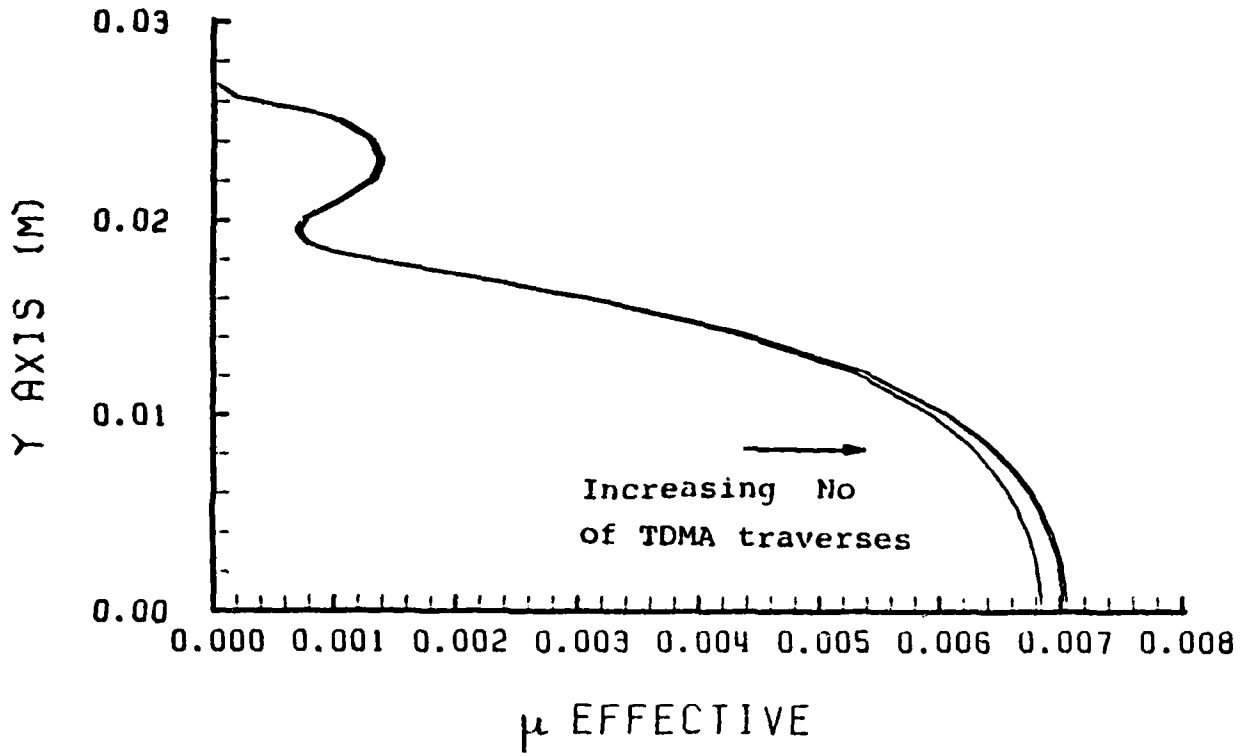

Figure 4.4. Effective Viscosity Distribution After the Second Sudden Enlargement, Changing the Number of TDMA Traverses

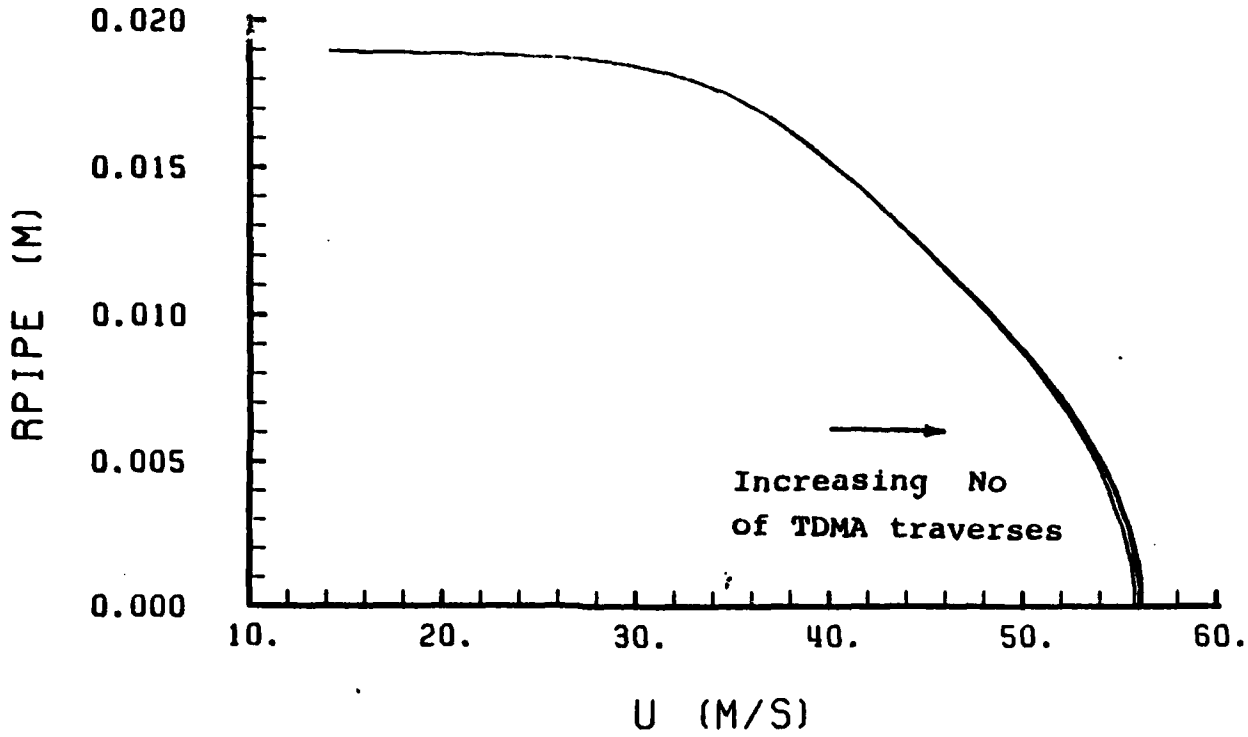

Figure 4.5. Axial Velocity Distribution After the First Sudden Enlargement, Changing the Number of TDMA Traverses

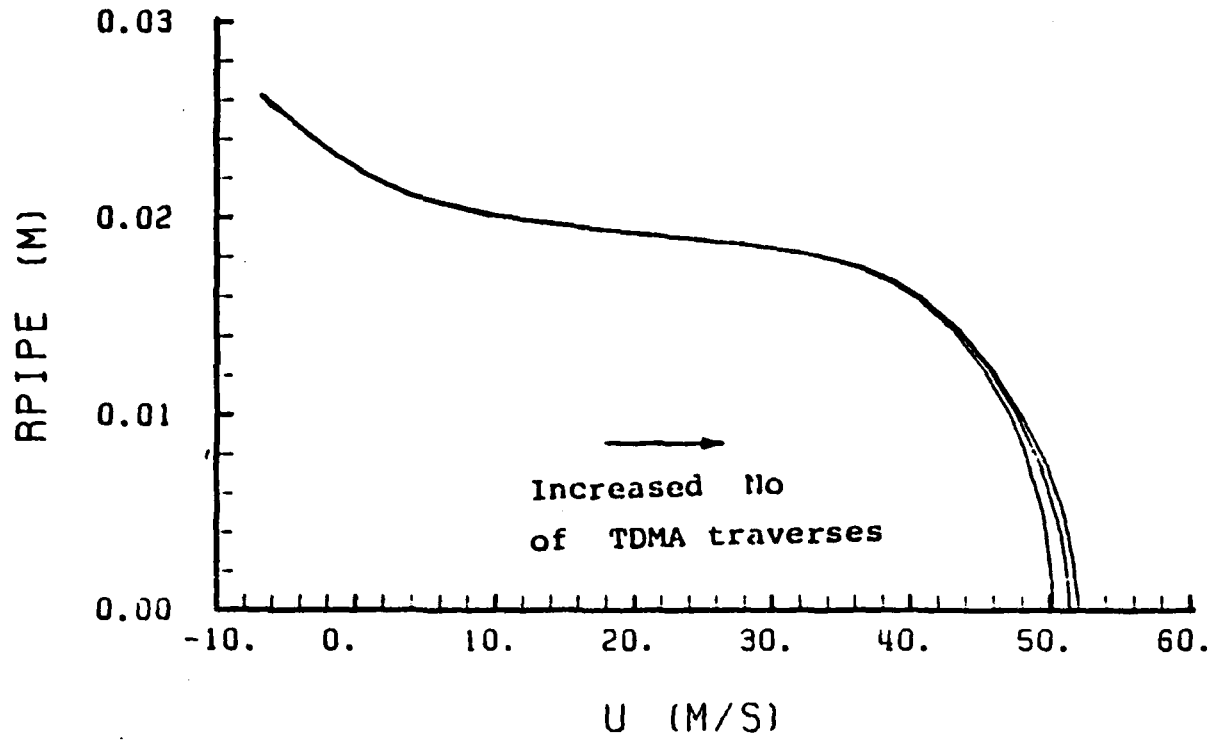

Figure 4.6. Axial Velocity Distribution After the Second Sudden Enlargement, Changing the Number of TDMA Traverses

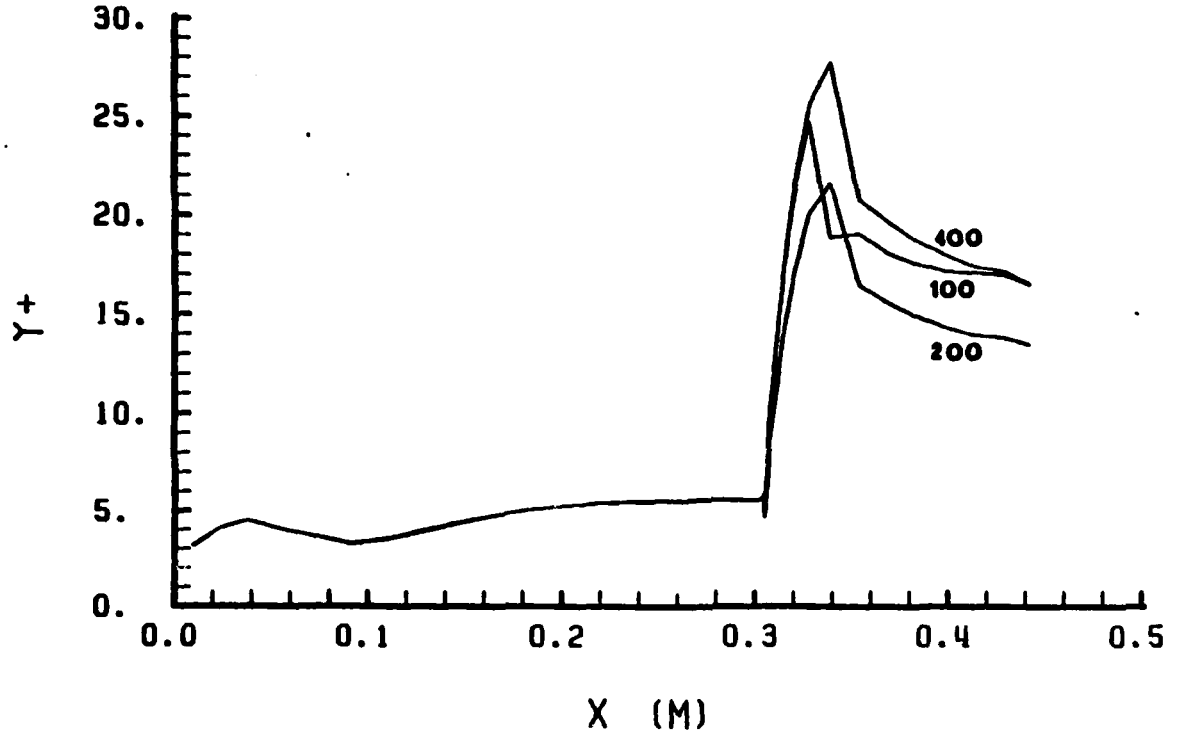

Figure 4.7. y_p^+ Distribution, Changing the Number of Sweeps

a change in the number of iterations did not significantly affect the y_p^+ distribution.

2. Temperature Distribution

The differences in the temperature distributions after the first sudden enlargement were negligible, as shown in Figure (4.8). The peak temperature, 2700°K, which was an indication of flame location, moved almost to the mid-radius point. Then, a relatively steep reduction of temperature occurred, and at the centerline its value was less than 2000°K.

After the second sudden enlargement, the temperature distribution differences were also negligible, as shown in Figure (4.9). The peak temperature now occurred at the centerline of the SFRJ, which meant that the enlargement effectively promoted the mixing of oxygen and unburned fuel.

3. Effective Viscosity Distribution

Figure (4.10) shows that the variations in effective viscosity distributions after the first sudden enlargement were almost negligible. All three curves coincided close to the solid fuel grain wall and then had a small separation as they approached the centerline. The same effect can be seen in Figure (4.11). These small differences in μ_{eff} close to the centerline did not really affect the calculations since, as will be seen later, the axial velocity distribution close to the centerline was amost uniform. As a result, the shear stress value was also low and was not affected by the variations

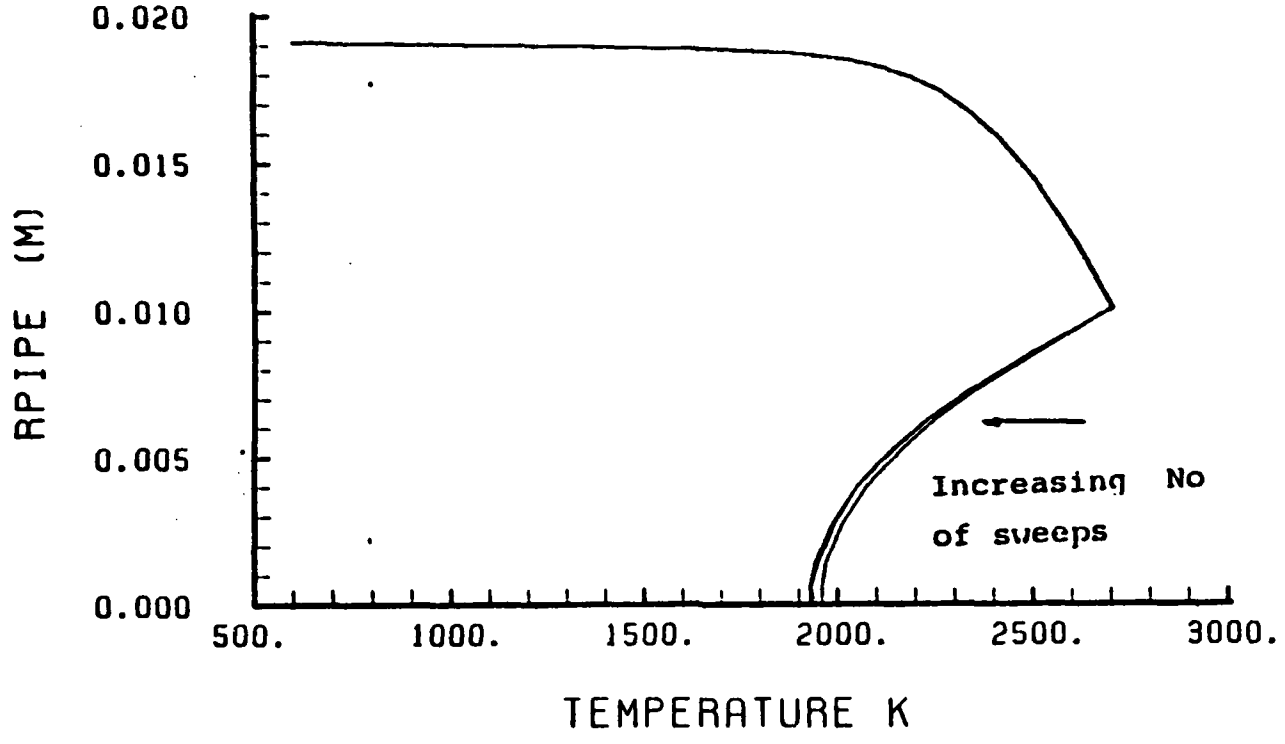

Figure 4.8. Temperature Distribution After the First Sudden Enlargement, Changing the Number of Sweeps

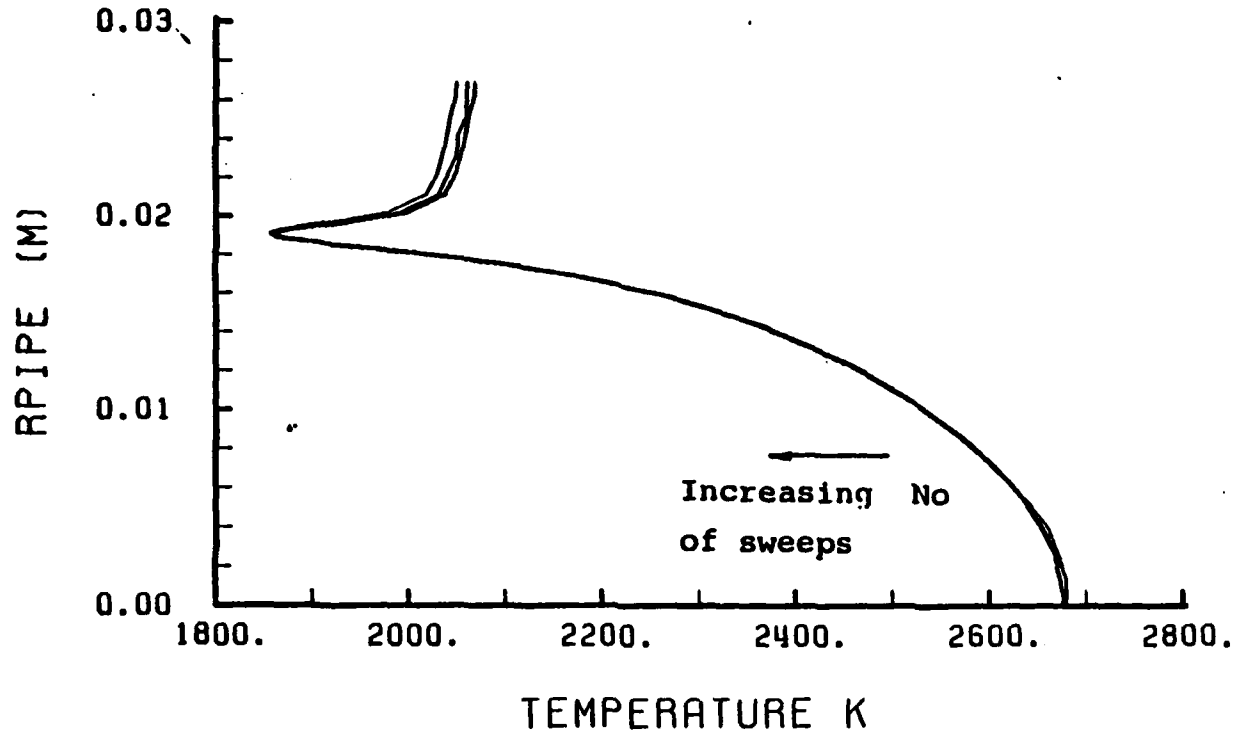

Figure 4.9. *Temperature Distribution After the Second Sudden Enlargement, Changing the Number of Sweeps*

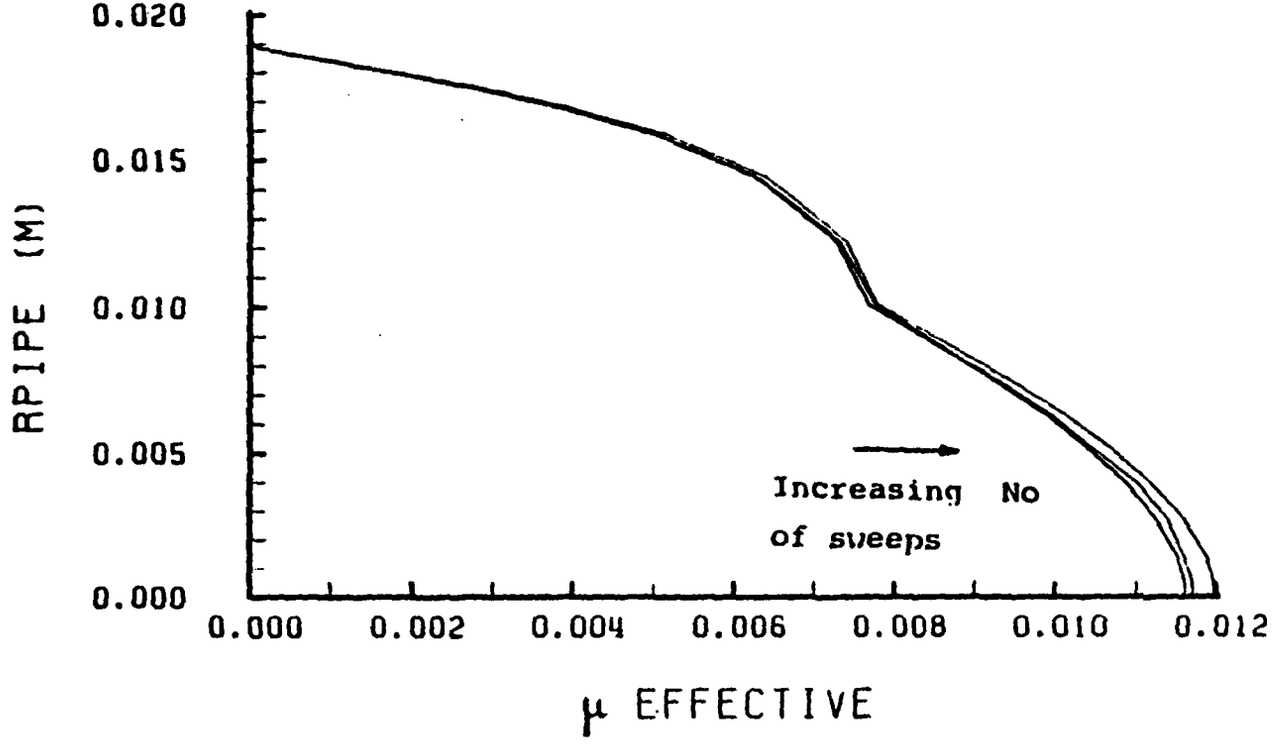

Figure 4.10. Effective Viscosity Distribution After the First Sudden Enlargement, Changing the Number of Sweeps

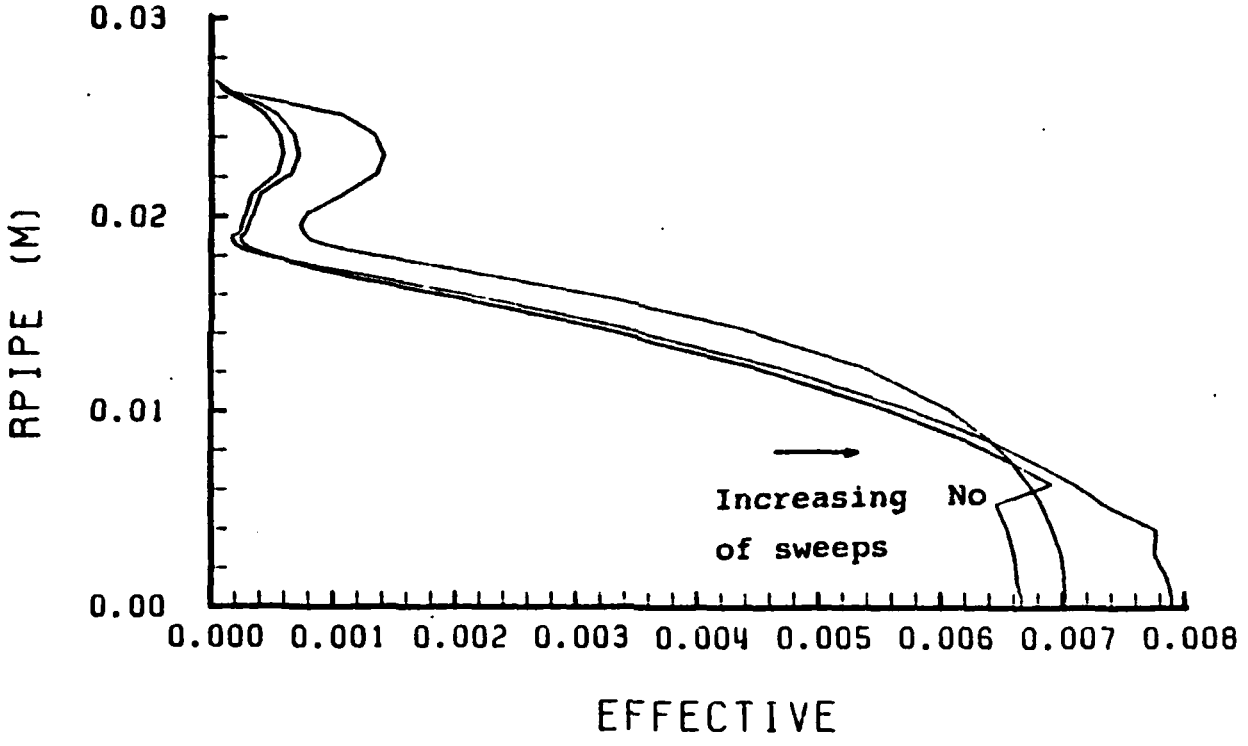

Figure 4.11. Effective Viscosity Distribution After the Second Sudden Enlargement, Changing the Number of Sweeps

of μ_{eff}. From the above, it is seen that a reduction in the number of sweeps to one half of the originally specified value did not significantly affect the effective viscosity distribution.

4. Axial Velocity Distribution

As for temperature and effective viscosity distributions, the variations in the distribution of axial velocity were also negligible for this range of iterations. Close to the solid fuel grain wall, the values of axial velocity were the same in all three cases. Close the centerline there was a separation, with higher values attained for higher numbers of iterations for both of the areas after the first and the second enlargement (shown on Figures (4.12) and (4.13), respectively).

Here, it was evident that increasing the number of iterations increased the accuracy attained; although, for this range of sweeps, the variation in the predictions did not exceed 3%.

D. EFFECT OF GRID SPACING CLOSE TO THE WALL

1. y_p^+ Distribution

The grid spacing was increased close to the solid fuel grain wall, such that turbulent conditions would exist at the near wall grid points all along the combustion length. The values of y_p^+ have been plotted in Figure (4.14). Values higher than 11.5 indicate turbulent flow, whereas lower values indicate laminar flow.

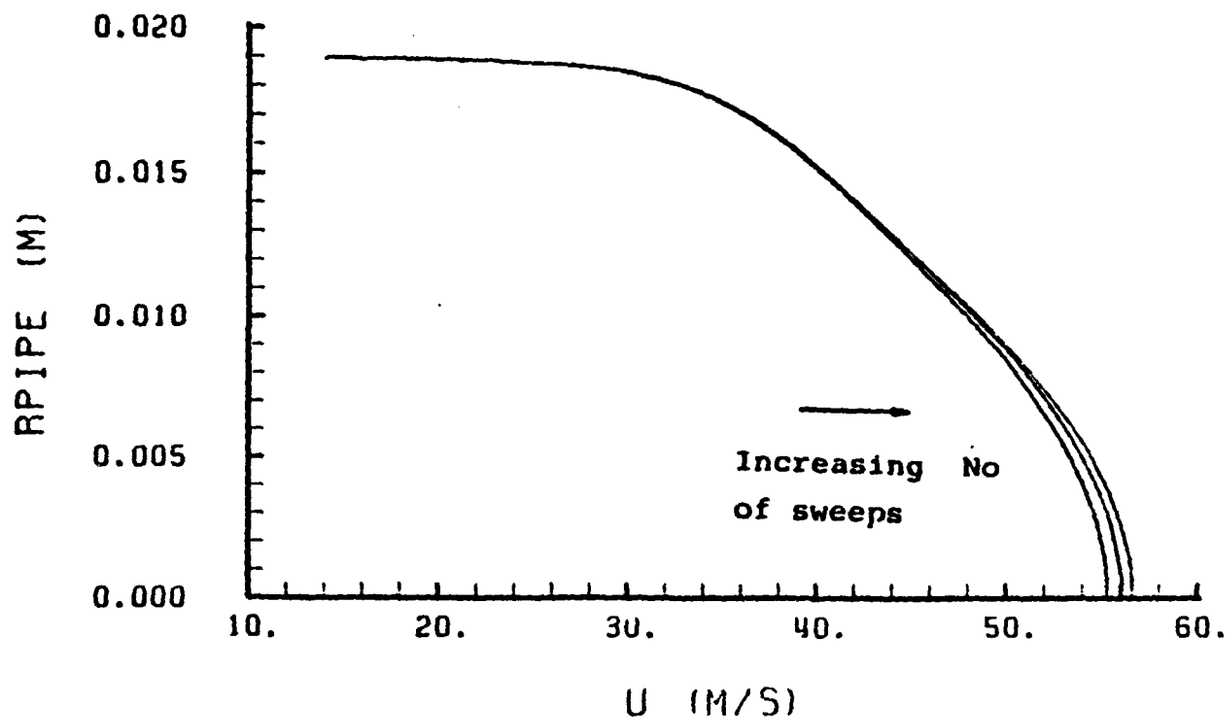

Figure 4.12. Axial Velocity Distribution After the First Sudden Enlargement, Changing the Number of Sweeps

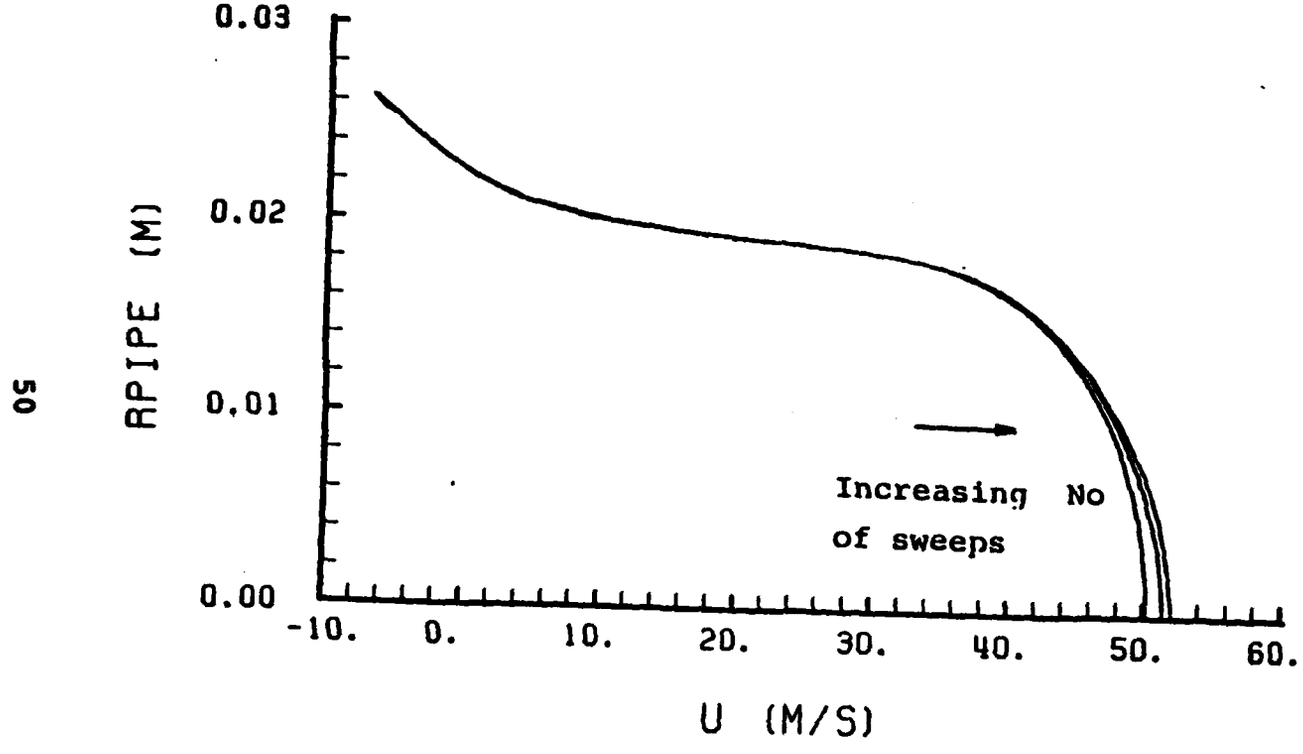

Figure 4.13. Axial Velocity Distribution After the Second Sudden Enlargement, Changing the Number of Sweeps

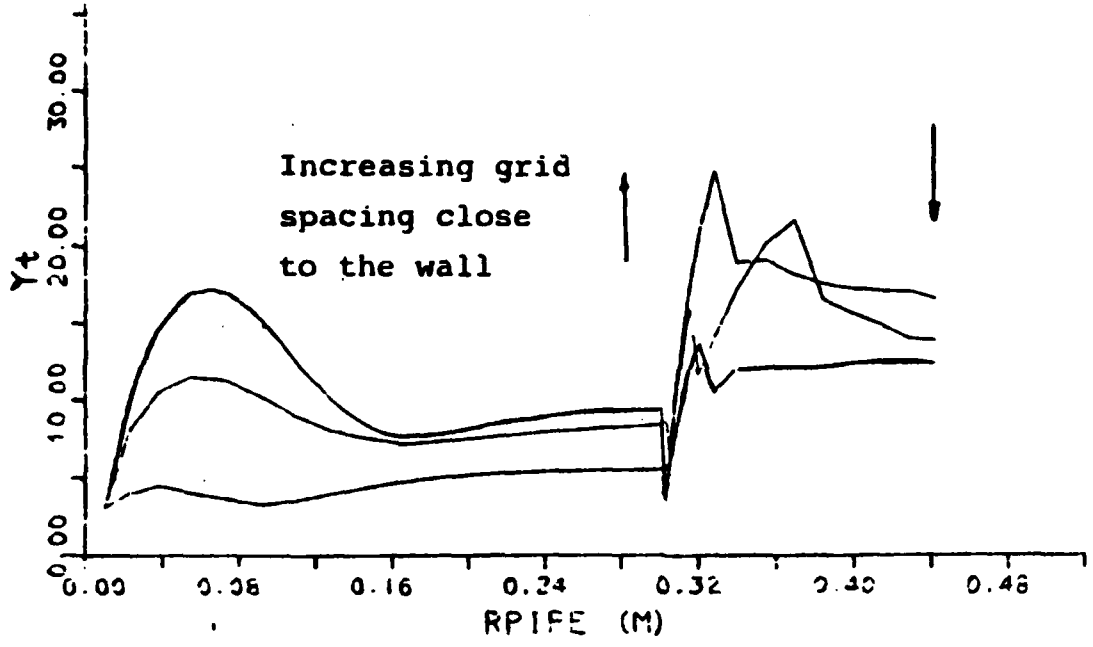

Figure 4.14. y_p^+ Distribution, Changing the Grid Spacing Close to the Solid Fuel Grain Wall

As shown on Figure (4.14), increasing the grid spacing close to the wall resulted in the values of y_p^+ being generally increased along the region from the first to the second sudden expansion. After the second sudden expansion, the values of y_p^+ that corresponded to increased grid spacing were generally lower, thus indicating less turbulence. However, the values were greater than 11.5 and the flow was handled as turbulent from the second expansion to the exit.

2. Temperature Distribution

The temperature distribution was dramatically affected by the grid spacing close to the solid fuel grain wall (i.e., the distance from the first node to the wall). Figure (4.15) shows that the original program predicted a peak temperature rather far from the wall. On the other hand, the program with increased spacing from the wall predicted peak temperatures close to the wall (the larger the grid spacing, the closer the distance of peak temperature to the wall). A peak temperature farther from the wall means a thicker boundary layer and, in turn, a more fuel rich mixture ratio .

Figure (4.16) shows that the original program predicted complete mixing in the aft mixing chamber. Peak temperature had been predicted to be at the centerline of the SFRJ, whereas with increased spacing the peak temperature occurred just behind the step wall.

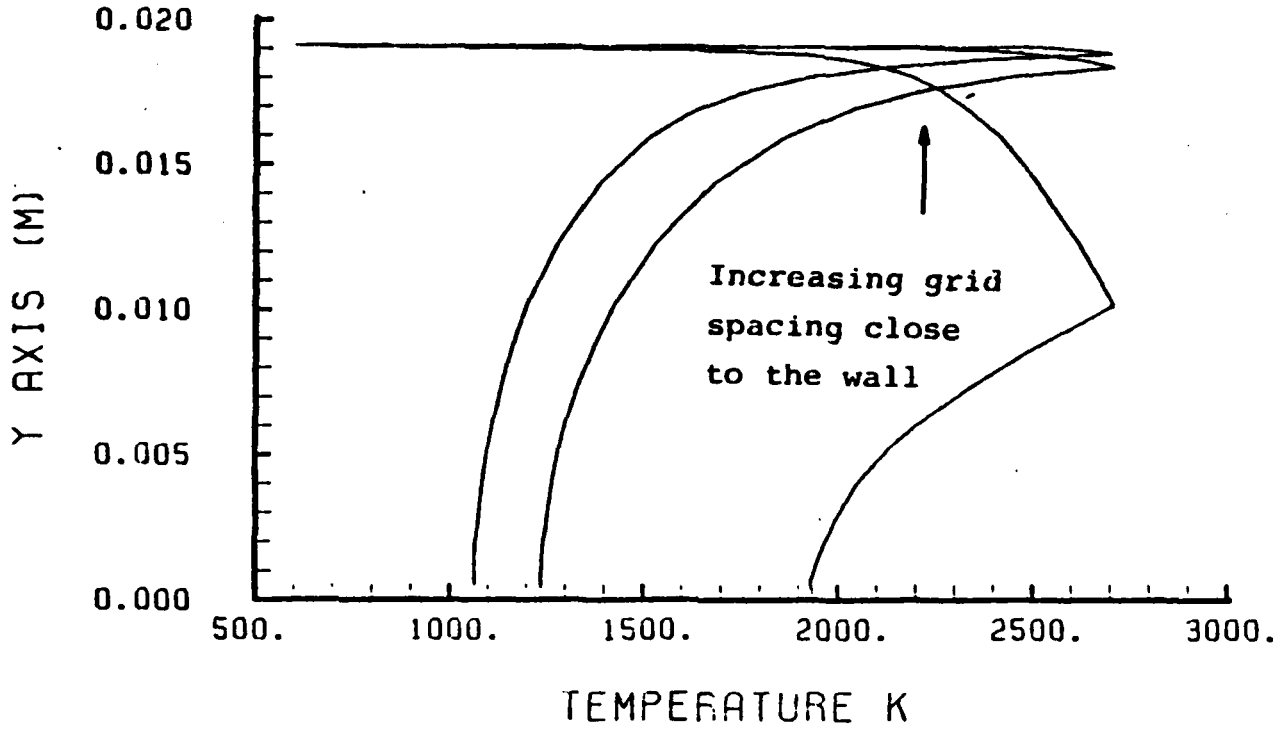

Figure 4.15. Temperature Distribution After the First Sudden Enlargement, Changing the Grid Spacing Close to the Wall

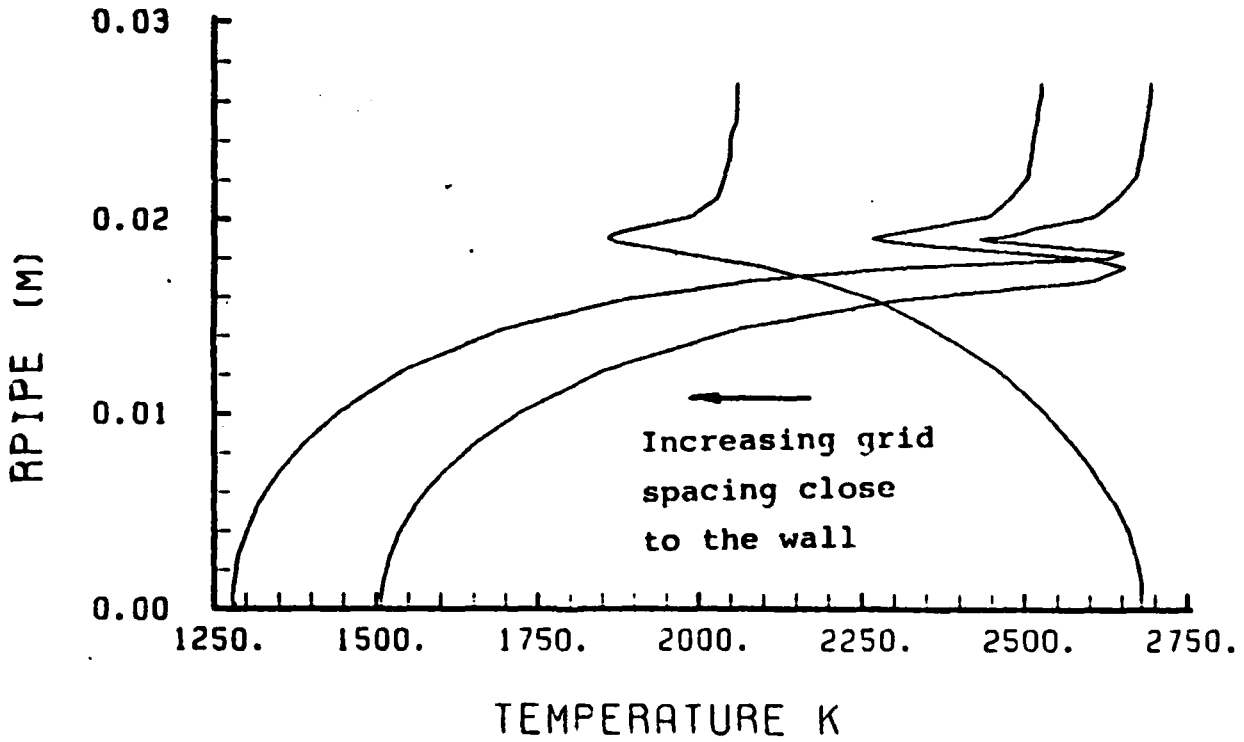

Figure 4.16. Temperature Distribution After the Second Sudden Enlargement, Changing the Grid Spacing Close to the Wall

3. Effective Viscosity Distribution

As shown on Figure (4.17), the effective viscosity distribution close to the well was not greatly affected by the spacing of the grid lines. However, close to the centerline the effective viscosity value increased with increasing spacing, while the value of μ_{eff} close to the wall was slightly greater in the original program.

The same happened after the second expansion, as shown on Figure (4.18), although the curves obtained were now somewhat different. Again, the effective viscosity from the original program was greater close to the wall, while, as the centerline was approached, this value dropped again below the values predicted for increased grid spacing close to the wall.

4. Axial Velocity Distribution

As shown on Figures (4.19) and (4.20), the original program predicted much higher velocities than the programs run with increased grid spacing close to the wall. It was also noted that the velocity profile of the original program was typical of laminar flow, where the ones for increased spacing were typical of turbulent flows (almost uniform velocity close to the core).

In this case too, the same general effects in the distribution could be noted as in those for effective viscosity. The original program predicted higher values than

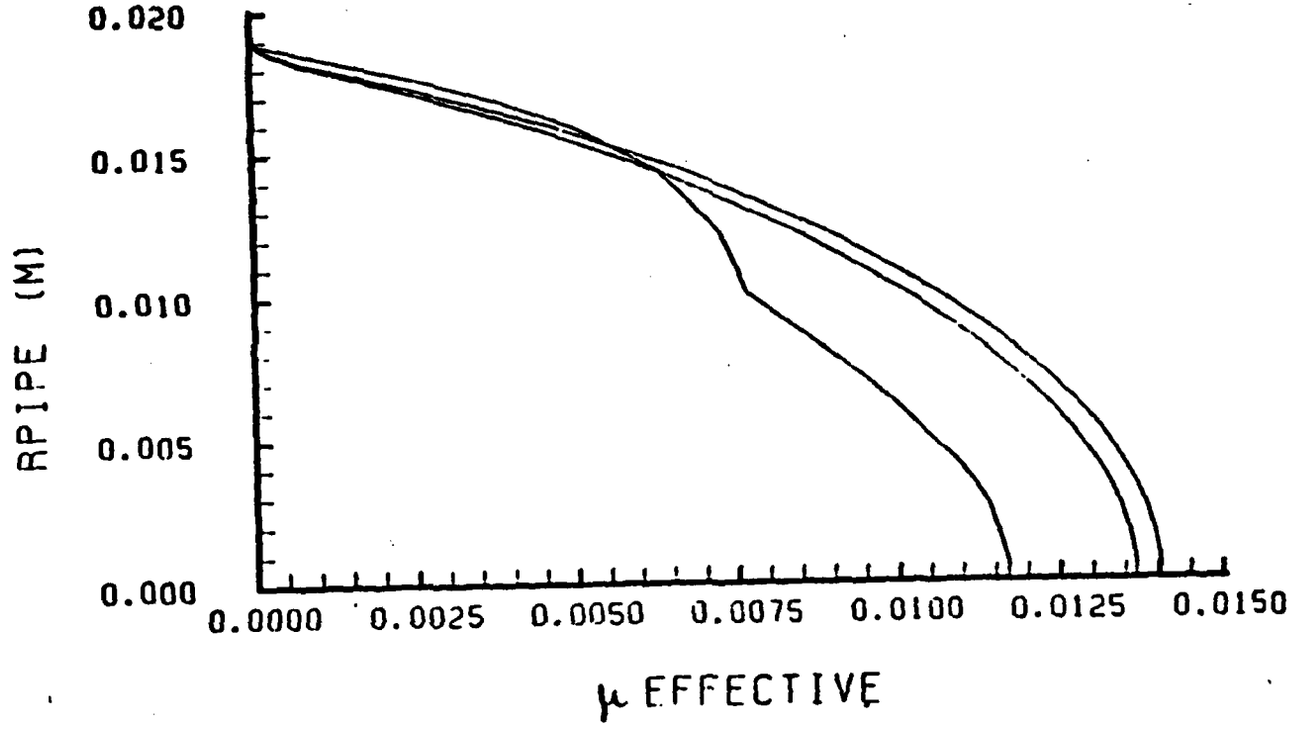

Figure 4.17. Effective Viscosity Distribution After the First Sudden Enlargement, Changing the Grid Spacing Close to the Wall

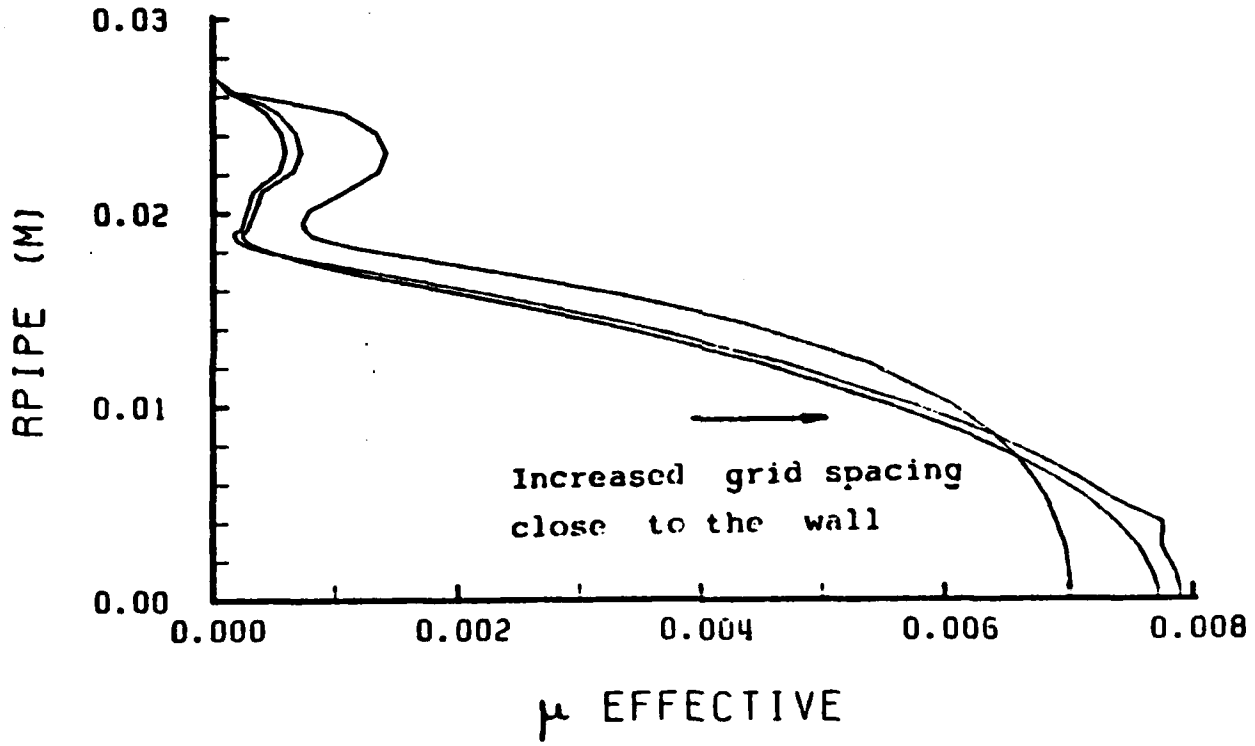

Figure 4.18. Effective Viscosity Distribution After the Second Sudden Enlargement, Changing the Grid Spacing Close to the Wall

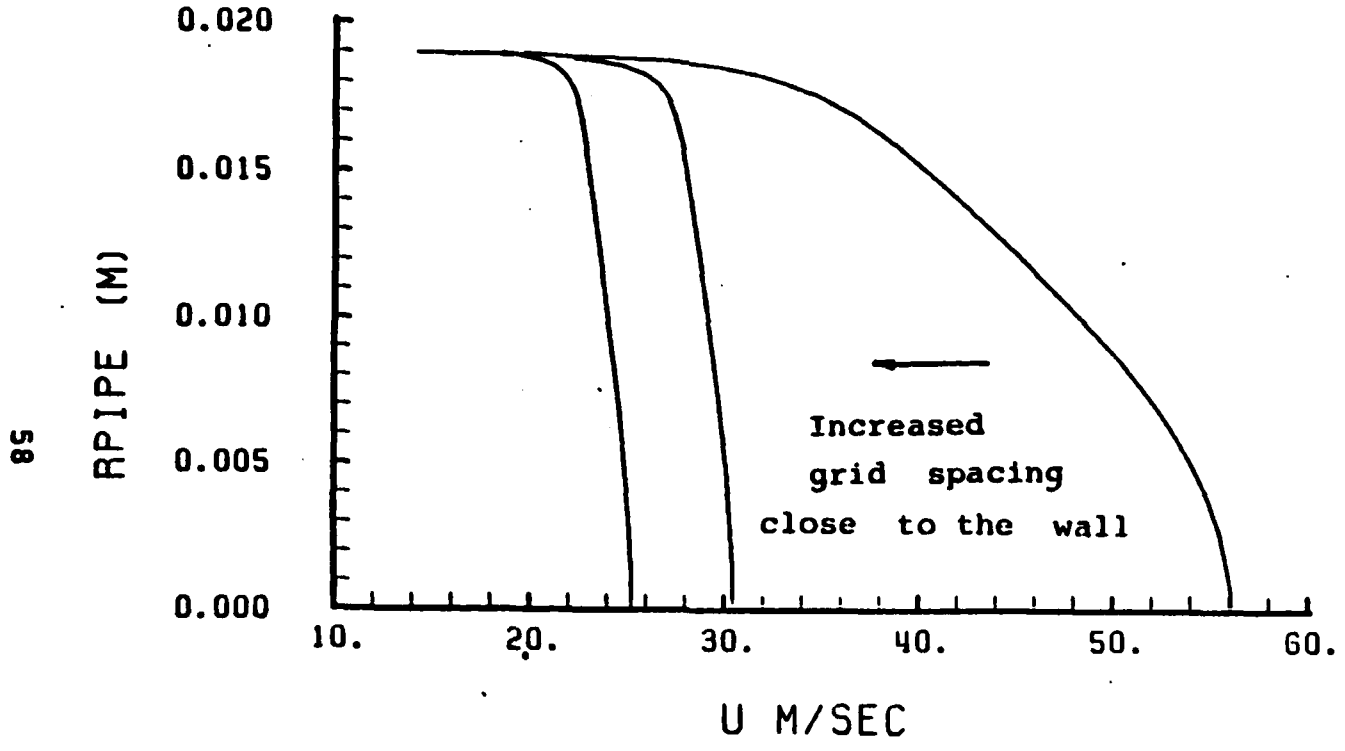

Figure 4.19. Axial Velocity Distribution After the First Sudden Enlargement, Changing the Grid Spacing Close to the Wall

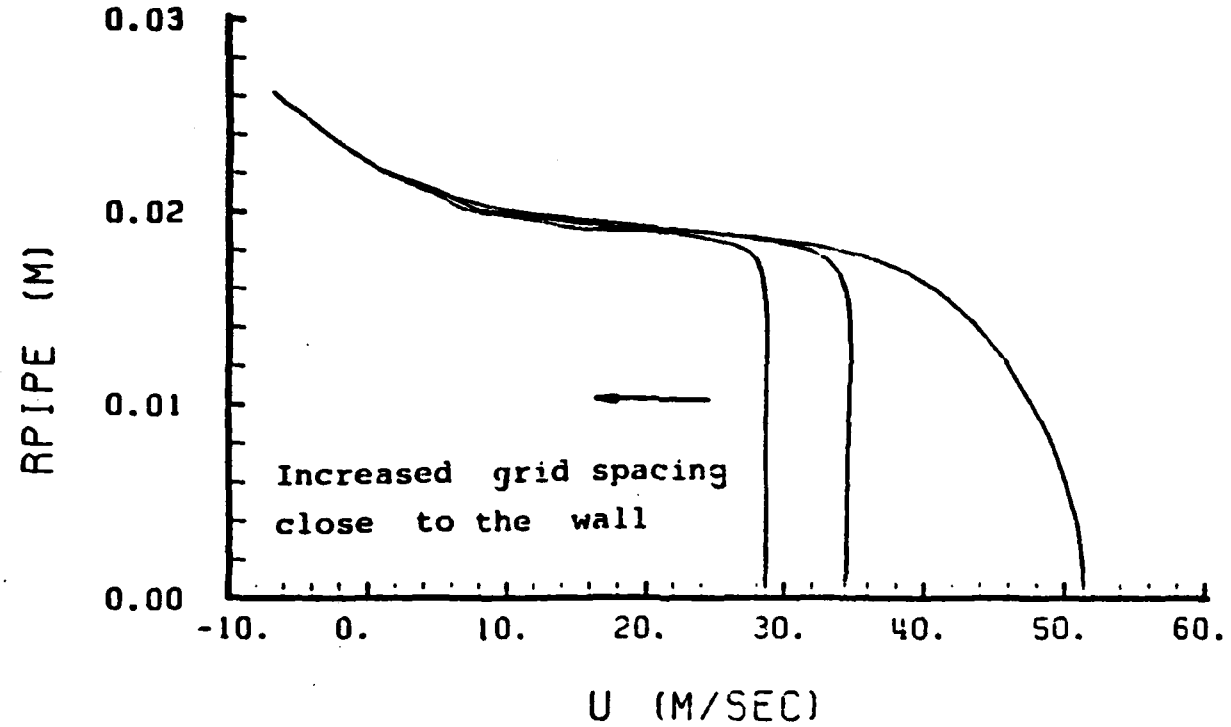

Figure 4.20. Axial Velocity Distribution After the Second Sudden Enlargement, Changing the Grid Spacing Close to the Wall

the programs with increased spacing and the velocity profiles corresponded to laminar and turbulent flows, respectively.

These large variations in the u-velocity distributions shown on Figures (4.19) and (4.20) were not surprising considering the variations in the temperature distributions. Since, for increased grid spacing, the temperature was lower in the core, the velocity was also lower than that obtained in the original program.

E. EFFECT OF A WIDER GRID SPACING

Since this case had similarities with the previous one, only one case was run; with increased grid spacing in both x and r directions. The y_p^+ vs. x distribution has been plotted, as shown on Figure (4.21). It was found that this case was not of particular interest. Along the solid fuel grain wall y_p^+ was slightly increased. This in turn meant that predictions would not be as accurate as those obtained increasing the grid spacing close to the wall only. So, no further analysis took place for this case.

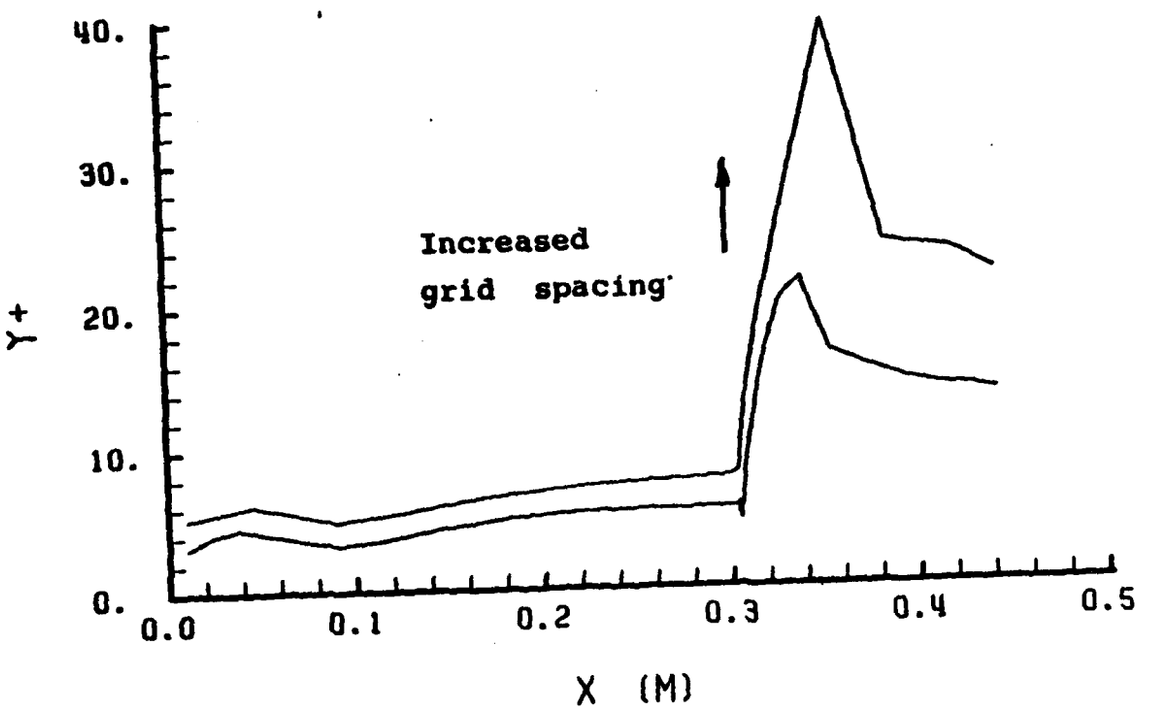

Figure 4.21. y_p^+ Distribution, Increasing the Grid Spacing in Both x and r Directions in the SFRJ

V. CONCLUSIONS

From the Analysis of Chapter IV it can be stated that:

a. The computer program was not sensitive to changes in the number of TDMA traverses, NTDMA. Thus, a lower value, such as NETDMA = 3 can be used without reducing the accuracy of predictions.

b. As expected, the higher the number of sweeps, LSWEEP, the greater the accuracy. However, if the number of iterations exceeded 200, the increase in accuracy was negligible. For any number of sweeps between 100 and 200, the accuracy of prediction was found to be very satisfactory.

c. The program was very sensitive in the grid spacing close to the solid fuel grain wall. For increased grid spacing in such a way as to have $y_p^+ > 11.5$ for most of the nodes adjacent to the solid fuel grain wall, the results of the program fit experimental data of Well [Ref. 5], as shown on Figure (5.1). Also, this increased spacing close to the wall permitted the reduction of the number of grid lines in the r and, consequently, the x-directions, with considerable savings in preparation as well as CPU time.

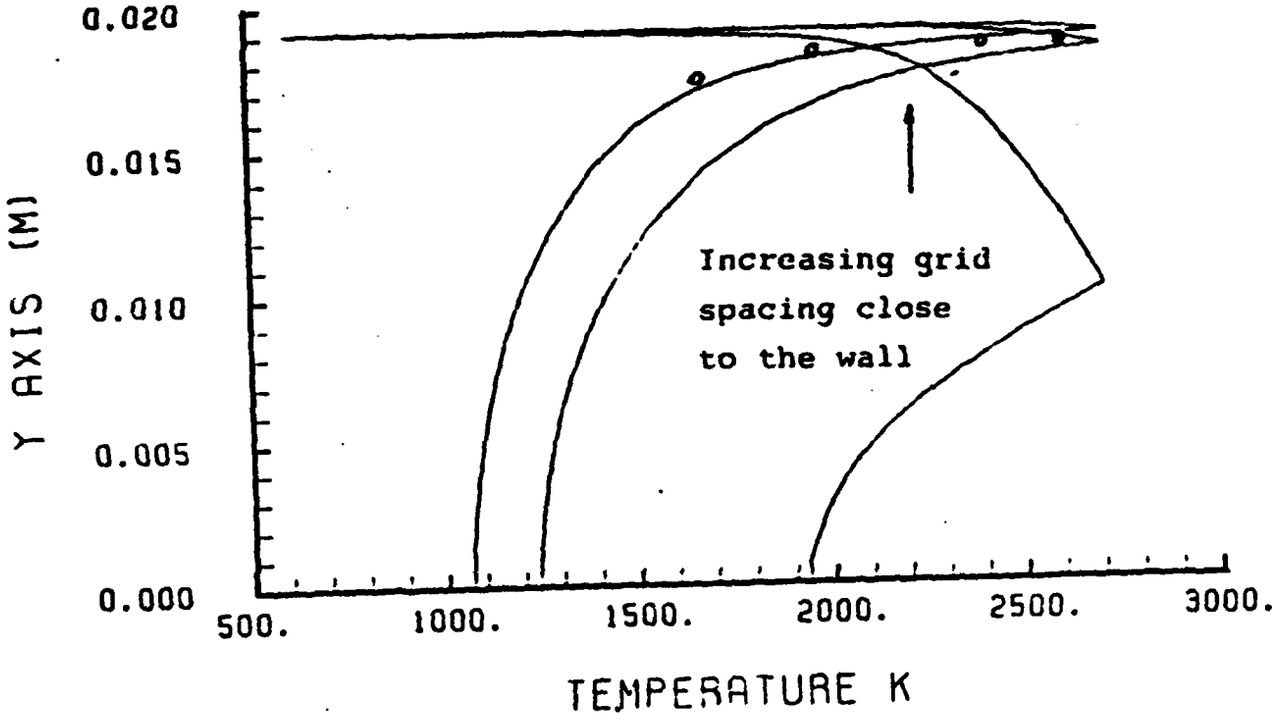

Figure 5.1. *Comparison of* Predicted Temperature Distribution with Experimental Data

VI. RECOMMENDATIONS

In view of the results of Chapters IV and V, the following are recommended, regarding the execution of the modified CHAMPION/2/E/FIX program.

a. The number of TDMA traverses should be reduced from five to three.

b. The number of iterations may remain the same or be reduced to one half without significant reduction in the accuracy of predictions. The use of any number of iterations greater than 200 is not expected to promote the accuracy significantly.

c. While establishing the grid, the nodes which are closer to the solid fuel grain wall should be selected in such a way as to result in values greater than 11.5 (at least for most of them). This will increase the accuracy of predictions and will enable the investigator to use fewer grid lines in both the x and y directions.

APPENDIX A

```
C/ASPI#5 JOB (3238,1085),'GENMIX',CLASS=C                          CHA00
C/*MAIN LINES=(12)                                                 CHA00
C/ EXEC FORTXCG,REGION=1024K                                       CHA00
C/FORT.SYSPRIN1 DD DUMMY                                           CHA00
C/FORT.SYSIN DD *                                                  CHA00
C ############################                                     CHA00
C ANDREA MH SVYSHS AYTO TO FAKELLO TON XREIAZOMAI GIA
     TH THESIS                                                     CHA00
C ################################                                 CHA00
      BLOCK DATA                                                   CHA00
      COMMON                                                       CHA00
     1/CASE51/RIN,IYIN,IYINP1,IXIN,IXINM1,TAULW(42),
       XPUSLW(42),CTAULW,                                          CHA00
     1  CXPLW                                                      CHA00
     1/CASE52/1XIN2,IYIN2,NXR1,NYR1,NXR1M1,NYR1M1,
       NYRIM2,                                                     CHA00
     1  CYPTW1,CTAUT1,CXPLW2,CTAUL2,HWALL2                         CHA00
     1/CASE1/UINLET,FLOWIN,RPIPE,XPIPE,FXSTEP,HINLET,
       HWALL                                                       CHA00
     2/DNY/ DYG(42),CYV(42),FV(42),FVNODE(42),R(42),
       RDYG(42),RDYV(42)                                           CHA00
     2,RSYG(42),RSYV(42),RV(42),RVCB(42),RVSQ(42),
       SYG(42),SYGTR(42)                                           CHA00
     2,SYV(42),SYVTRV(42),Y(42),YV(42)                           CHA00
     3/DNYONX/AE(42),AN(42),AP(42),AS(42),AW(42),C(42),
       D(42),DIFE(42)                                              CHA00
     3,DIFN(42),DUW(42),DIFW(42),DU(42),DV(42),EMUE(42),
       EMUN(42)                                                    CHA00
     3,EMUW(42),USTAR(42),VSTAR(42)                              CHA00
     3,PHIOLD(42),RHOE(42),RHON(42),RHOW(42),S(42),
       SPRIME(42)                                                  CHA00
     3,VOLUME(42),CONN(42),CONE(42),CONW(42)                     CHA00
     4/DNX/DXG(47),DXU(47),FAREA(47),FU(47)                      CHA00
     4,FUNODE(47),KOUNT(47),RDXG(47)                             CHA00
     4,RDXU(47),RSXG(47),RSXU(47),STORE(47),SXG(47),
       SXU(47),X(47),XU(47)                                        CHA00
      COMMON                                                       CHA00
     5/DJPHI/ IEW(IC),ILAST(10),IMON(10),IXNY(10),
       IZERC(10)                                                   CHA00
     5,KSOLVE(11),KRS(10),RELAX(10),RSREF(10),RSSUM(10),
       TITLE(10)                                                   CHA00
      COMMON                                                       CHA00
     6/DO/CCHECK,DP,FLOWPC,FLOWST,FLOWUP,GREAT,IPLRS,
       IPREF,IPRINT                                                CHA00
     6,IWEEEP,IX,IX1NY,IX1NY1,IX2NY2,IXMON,IXP1,IXPREF,
       IXU,IYMON,IYPREF                                            CHA00
```

```
     6,JEMU,JH,JLAST,JP,JPP,JRHO,JU,JV,JVP1,KALLED,
       KINPRI,KEHOMU                                                    CHA00
     6,KTEST,LABPHI,LSWEEP,NSOLVE,NTRAV,KRAD                          CHA00
     6,IYF,IYF1,IYL,IYLM1,IYLP1,NTDMA,NUMCOL                          CHA00
     6,N),NXMA),NXM1,NXM2,NXYG,NXYP,NXYU,NXYV                         CHA00
     6,NYNYMA),NYM1,NYM2,PI,RSCHEK,RSMAX,TINY                         CHA00
     6,IPFRS1,IPFRS2,KIN,KEX                                          CHA00
      COMMON/PROP,EMUREF,PREFF(10),PRL(10),PRT(10),
       RHOREF                                                         CHA00
      COMMON/D2D1/ARSL(47,10),RSLINE(47,10)                           CHA00
      COMMON/D2D2/U(1560),V(1560),TKE(1600),TED(1600),
       H(1600),PP(40),                                                CHA00
     7P(1444),RHO(1600),EML(1600),RSF(40,40),T(1600)                  CHA00
      DIMENSION F(14200)                                              CHA00
      COMMON                                                          CHA00
     9/TURB/C1,O2,CD,SCRTCD,CD25,ECONST,CTAUTW,CYPTW,
       TAUTW(47),GENK(42),                                            CHA00
     9YPUSTW(47),FACTKE,FACTED,JTKE,JTED,CAPPA,STANTW(47),
       HBULK(47),                                                     CHA00
     9RUN,CP,GC,HINR,HWALLR,PREFR,BARM,JT,HOHECK                      CHA00
     9/COMB/AWALL(42),FLUX(42),FLOWAL(42),BP(42),
       RR(42),TEMP1(42),                                              CHA00
     9EMUF,RHCF,HUF,HTR,TREF,STC,HC,FN2IN,FOXIN,                      CHA00
     9FMCLFU,FMCLPR,FMCLOX,FMOLN2                                     CHA00
     9/CHEMCO/FFU(42),FOX(42),FN2(42),                                CHA00
     9FLFUIT,FLFLOT,FLOXIT,FLOXCT,FLN2IT,FLN2)T,                      CHA00
     9PCEFU,PCECX,PCEN2,RRAVE,LINE                                    CHA00
      REAL*8 TL(12)                                                   CHA00
      LOGICAL*1 LTG(3).                                               CHA00
      COMMON                                                          CHA00
     D/OPLOT/TL                                                       CHA00
     D,KPLOT(11),NINT(11),PHI(40,40),CL(25),XP(47),
       SCALEW,SCALEH,LTG                                              CHA00
      COMMON/RAD/TWALL,TFLAME,SIGMA,EPSIW,IRAD                        CHA00
     E,IRADS,RAD1,FUEL(40),QRAD(40),QCON(40),FMASF(40),
       VOLL(40)                                                       CHA00
      DIMENSION DIFS(42),EMUS(42),RHOS(42),CONS(42)                   CHA00
      EQUIVALENCE(CONS(2),CONN(1))                                    CHA00
      EQUIVALENCE (DIFS(2),DIFN(1)), (EMUS(2),EMUN(1))                CHA00
C     EQUIVALENCE (RHOS(2),RHON(1)),(AREAE,AREAW)                     CHA00
      EQUIVALNECE (RHOS(2),RHON(1))                                   CHA00
      EQUIVALENCE (F(1),U(1))                                         CHA00
      DIMENSION A(42),B(42)                                           CHA00
      EQUIVALENCE(A(1),AN(1)),(B(1),AS(1))                            CHA00
CHAPTER  1-------------- GENERAL,FLOW PARAMETERS                       CHA00
      DATA GREAT,TINY,PI/1.E30,  1.E-30, 3.1415926/                   CHA00
C                                                                     CHA00
      DATA RPIPE,XPIPE,UINLET,HINLET,HWALL/                           CHA00
     10.026924,0.4628,92.220,0.0,1.0/                                 CHA00
C                                                                     CHA00
C                                                                     CHA00
      DATA HWALL2/1.0/                                                CHA00
      DATA IXIN,IYIN/2,7/                                             CHA00
```

```
      DATA IXIN,IYIN/2,7/                                              CHA00
C     DATA KTEST/0/                                                    CHA00
      DATA KTEST/1/                                                    CHA00
CHAPTER 2 -------------- GRID                                          CHA00
      DATA NXMAX,NYMAX/40,40/                                          CHA00
C                                                                      CHA00
      DATA NX,NY/40,33/                                                CHA00
      DATA KRAD/2/                                                     CHA00
C     KRAD=2 MEANS CYLINDRICAL POLAR COORDINATES.                      CHA00
C     IF ONE WISHES THE PROGRAM TO CALCULATE THE GRID,                 CHA00
C      SET X(1) OR Y(1) NOT EQUAL TO 0.0                               CHA00
C                                                                      CHA00
C                                                                      CHA00
      DATA X/0.0,.01,.023,.038,.055,.07333,.09166,
       .10999,.12832,                                                  CHA00
     A.14665,.16498,.18331,.20164,.21997,.2383,.25663,
       .27343,.28468                                                   CHA00
     B.29218,.29718,.30055,.3028,.3043,.3053,                         CHA00
     C.3066,.3081,.3096,.31185,.31522,.32022,.32772,
       .33892,.35392,                                                  CHA00
     D.36892,.38292,.39892,.41392,.42892,.44192,
       .4543,.4643,                                                    CHA00
     E0.,0.,0.,0.,0.,0./                                              CHA00
      DATA Y/0.0,.00061,.00141,.00271,.00401,.00531,
       .00631,.00731,                                                  CHA00
     A.00861,.01011,.012235,.01436,.01586,.01686,
       .01753,.01798,.01828,                                           CHA00
     B.01853,.01873,.01888,.01900,.01910,.01925,                      CHA00
     C.01955,.02015,.02112,.02215,.02315,.02415,.02515,               CHA01
     D.02565,.026260,.026924,0.,0.,0.,0.,0.,0.,0.,0.,0./              CHA01
C                                                                      CHA01
      DATA FXSTEp/1.5/                                                 CHA01
CHAPTER 3 --------------- VARIABLES                                    CHA01
C------ VARIABLES SOLVED BY TDMA                                      CHA01
      DATA JU,JV,JTKE,JTED,JH,JPP/1,2,3,4,5,6/                         CHA01
C------ AUXILIARY VARIABLES                                           CHA01
      DATA JP,JRHO,JEMU,JT,JLAST/7,8,9,10,10/                          CHA01
C------ THE NUMBER OF DEPENDENT VARIABLES SOLVED                      CHA01
      DATA NSOLVE/5/                                                   CHA01
      DATA KSOLVE/9*1,2*0/                                             CHA01
      DATA KRS/6*1,4*0/                                                CHA01
C                                                                      CHA01
      DATA RELAX/0.3,0.3,0.5,0.5,1.,1.,0.1.,01,0.5,1./                 CHA01
      DATA TITLE/10*4HXXXX/                                            CHA01
CHAPTER 4 -------------- PROPERTY DATA                                 CHA01
      DATA RHOREF,EMUREF/1.403,3.034E-5/                               CHA01
      DATA PRL,PRT/12*1.,  .9,  7*1./                                  CHA01
      DATA PREFF/3*1.0,  1.3,  6*1.0/                                  CHA01
      DATA C1,C2,CD,CAPPA,ECONST/1.43,1.92,0.09,0.4,9.0/               CHA01
C     EPSIW IS WALL EMISSIVITY,RAD1 IS EMP.CONST.FOR                   CHA01
C     EMISSGAS/UNBURNED FUEL ON A LINE                                 CHA01
      DATA SIGMA,EPSIW,TWALL,TFLAME,RAD1/                              CHA01
```

```
     15.669E-08,0.85,600.,3190.,3.0000/                              CHA01
C     IRAD=0,BP NOT MODIFIED FOR RADIATION                           CHA01
C     IR/D=1 WITH RADIATION                                          CHA01
      DATA IRAD/0/                                                   CHA01
C     DATA IRAD/1/                                                   CHA01
CHAPTER 5 -------------- STARTING PREPARATIONS                       CHA01
      DATA IXPREF,IYPREF/2,2/                                        CHA01
      DATA IXMON,IYMON/22,24/                                        CHA01
      DATA KINPRI/0/                                                 CHA01
      DATA F,DV/14200*0.0,42*0.0/                                    CHA01
      DATA FACTKE,FACTED/0.005,0.03/                                 CHA01
CHAPTER 6 --------------- STEP CONTROL                               CHA01
CHAPTER 7 -------------- BOUNDARY CONDITIONS                        CHA01
      DATA KIN,KEX/3,1/                                              CHA01
CHAPTER 8 -------------- ADVANCE                                    CHA01
      DATA NTDMA/5/                                                  CHA01
      DATA RSCHEK/0.001/                                             CHA01
CHAPTER 9 -------------- COMPLETE                                   CHA01
C                                                                    CHA01
C     SUBROUTINE DENSIT CALCULATES VARIABLE DENSITY
       ON EACH LINE.                                                 CHA01
C     RUN=UNIVERSAL GAS CONSTANT                                     CHA01
C      CP=C SUB P                                                    CHA01
C      PREFR IS THE REFERENCE PRES ADDED TO P(I) TO
       CALCULATE P ACTUAL                                            CHA01
C                                                                    CHA01
      DATA FLOWAL/42*0.0/                                            CHA01
      DATA RUN,OP,GC/8314.0,1004.0,1.0/                              CHA01
C                                                                    CHA01
      DATA HINP,HWALUR,PREFR,BARM/2.6570E06,4.826E05,
       3.152E05,28.964/                                              CHA01
      DATA HTR,FOXIN,FN2IN,STC,HC/2.300E16,0.233,
       0.767,1.92,2.443E07/                                          CHA01
      DATA FMOLFU,FMCLPR,FMOLOX,FMOLN2/100.0,28.97,
       32.0,28.0/                                                    CHA01
      DATA RHOF,EMUF/1199.,2.43E-05/                                 CHA01
      DATA TREF/600.0/                                               CHA01
C                                                                    CHA01
C     SET VARIABLE 'LINE' = IX ON THE LINE ON WHICH
C      CONSERVATION CALCULATIONS DESIRED.                            CHA01
      DATA LINE/29/                                                  CHA01
C                                                                    CHA01
CHAPTER 10 ------------ ADJUST                                       CHA01
CHAPTER 11 ------------- PRINT                                       CHA01
      DATA NUMCOL/10/                                                CHA01
      DATA IPLRS,IPRINT/200,200/                                     CHA01
C ### CORRECTION ON BASIC PROGRAM ###                                CHA01
      DATA IPLRS,IPRINT/200,200/                                     CHA01
CHAPTER 12 ------------ DECIDE                                       CHA01
      DATA CCHECK/0.001/                                             CHA01
      DATA LSWEEP.200/                                               CHA01
```

```
C##########################################                    CHA01
C     DATA LSWEEP/2/                                          CHA01
C##########################################                    CHA01
C                                                             CHA01
          END                                                 CHA01
C     PROGRAM MAIN(OUTPUT,TAPE6=OUTPUT)                       CHA01
C-------------------------------------------------------------CCHa01
C  FOR CHAMPION 2/E/FIX,CASE50,(HTS7628,C50)                  CHA01
C   IDENT CASE51                                              CHA01
C  29.7,77                                                    CHA01
C                                                             CHA01
C-------------------------------------------------------------CCHA01
C                                                            CCHA01
C/JULY 1977/                                                 CCHA01
C                                                            CCHA01
C        A DETAILED DESCRIPTION OF THE PROGRAM CAN BE        CCHA01
C        FOUND IN THE REPORT  A GENERAL COMPUTER             CCHA01
C        PROGRAM FOR TWO-DIMENSIONAL ELLIPTIC FLOWS          CCHA01
C        BY W.M. PUN AND D.B. SPALDING, HTS/76/2,            CCHA01
C        MECHANICAL ENGINEERING DEPARTMENT, IMPERIAL         CCHA01
C        COLLEGE, LONDON                                     CCHA01
C                                                            CCHA01
C                                                            CCHA01
C-------------------------------------------------------------CCHA01
CHAPTER 0  0  0  0  0  0  0  0  0  DECLARATIONS 0  0  0      CHA01
C                                                             CHA01
      COMMON                                                  CHA01
     1/CASE51/RIN,IYIN,IYINP1,IXIN,IXINm1,TAULW(42),
       XPUSLW(42),CTAULW,                                     CHA01
     1  CXPLW                                                 CHA01
     1/CASE52/IXIN2,IYIN2,NXR1,NYR1,NXR1M1,NYR1M1,
       NYR1M2,                                                CHA01
     1  CYPTW1,CTAUT1,CXPLW2,CTAUL2,HWALL2                    CHA01
     1/CASE1/UINLET,FLOWIN,RPIPE,XPIPE,FXSTEP,HINLET,
       HWALL                                                  CHA01
     2/DNY/ DYG(42),DYV(42),FV(42),FVNODE(42),R(42),
       RDYG(42),RDYV(42)                                      CHA02
     2,RSYG(42),RSYV(42),RV(42),RVCB(42),RVSQ(42),
       SYG(42),SYGTR(42)                                      CHA02
     2,SYV(42),SYVTRV(42),Y(42),YV(42)                        CHA02
     3/DNYONX/AE(42),AN(42),AP(42),AS(42),AW(42),C(42),
       D(42),DIFE(42)                                         CHA02
     3,DIFN(42),DUW(42),DIFW(42),DU(42),DV(42),EMUE(42),
       EMUN(42)                                               CHA02
     3,EMUW(42),USTAR(42),VSTAR(42)                           CHA02
     3,PHIOLD(42),RHOE(42),RHON(42),RHOW(42),S(42),
       SPRIME(42)                                             CHA02
     3,VOLUME(42),CONN(42),CONE(42),CONW(42)                  CHA02
     4/DNX/DXG(47),DXU(47),FAREA(47),FU(47)                   CHA02
     4,FUNODE(47),KOUNT(47),RDXG(47)                          CHA02
     4,RDXU(47),RSXG(47),RSXU(47),STORE(47),SXG(47),
       SXU(47),X(47),XU(47)                                   CHA02
```

```
5/DJPHI/ IEW(10),ILAST(10),IMON(10),IXNY(10),
  IZERO(10)                                                    CHA02
5,KSOLVE(11),KRS(10),RELAX(10),RSREF(10),RSSUM(10),
  TITLE(10)                                                    CHA02
 COMMON                                                        CHA02
6/DO/CCHECK,DP,FLOWPC,FLOWST,FLOWUP,GREAT,IPLRS,
  IPREF,IPRINT                                                 CHA02
6,ISWEEP,IX,IX1NY,IX1NY1,IX2NY2,IXMON,IXP1,IXPREF,
  IXU,IYMON,IYPREF                                             CHA02
6,JEMU,JH,JLAST,JP,JPP,JRH0,JU,JV,JVP1,KALLED,
  KINPRI,KRHOMU                                                CHA02
```

LIST OF REFERENCES

1. Netzer, D.W., "Modeling Solid-Fuel Ramjet Combustion," Journal 77 of Spacecraft and Rockets, Vol. 14, Dec 1977, pp. 672-766.

2. Stevenson, C.A., Netzer, D.W., "Primitive Variable Model Applications to Solid Fuel Ramjet Combustion," Journal of Spacecraft and Rockets, Vol. 18, Jan-Feb 1981, pp. 89-94.

3. Pun, W.M., Spalding, D.B., A General Computer Program for Two-Dimensional Elliptic Flows, Imperial College of Science and Technology, 1977.

4. Jones, W.P., Launder, B.E., The Prediction of Laminarization With a Two-Equation Model of Turbulence, Pergamon Press, 1972.

5. Netzer, D.W., Model Applications to Solid-Fuel Ramjet Combuation, AIAA, 1978.

6. Naval Postgraduate School, NPS67-81-012, Modeling Solid-Fuel Ramjet Combustion Including Radiation Heat Transfer to the Fuel Surface, Netzer, D.W., Metochianakis, M.E., et al, 1980.

BIBLIOGRAPHY

Kayes, W.M., Convective Heat and Mass Transfer, McGraw-Hill, 1966.

Ketter, R.L., Prawel, S.P., Modern Methods of Engineering Computation, McGraw-Hill, 1969.

INITIAL DISTRIBUTION LIST

		No. of Copies
1.	Defense Technical Information Center Cameron Station Alexandria, Virginia 22314	2
2.	Library, Code 0142 Naval Postgraduate School Monterey, CA 93943	2
3.	Department Chairman, Code 67 Department of Aeronautics Naval Postgraduate School Monterey, CA 93943	1
4.	Professor. H.W. Burden, Code 67Zx Department of Aeronautics Naval Postgraduate School Monterey, CA 93943	2
5.	Professor D.W. Netzer, Code 67Nt Department of Aeronautics Naval Postgraduate School Monterey, CA 93943	1
6.	Capt. P.D. Vidos KETA, T.G.A. 1010 Palaion Faliron Athens, Greece	1
7.	Capt. A.S. Pilos 37 Kyrenia St. Papagou, Greece	2
8.	Captain Z.Z. Gikas SMC 2543 Naval Postgraduate School Monterey CA 93943	1

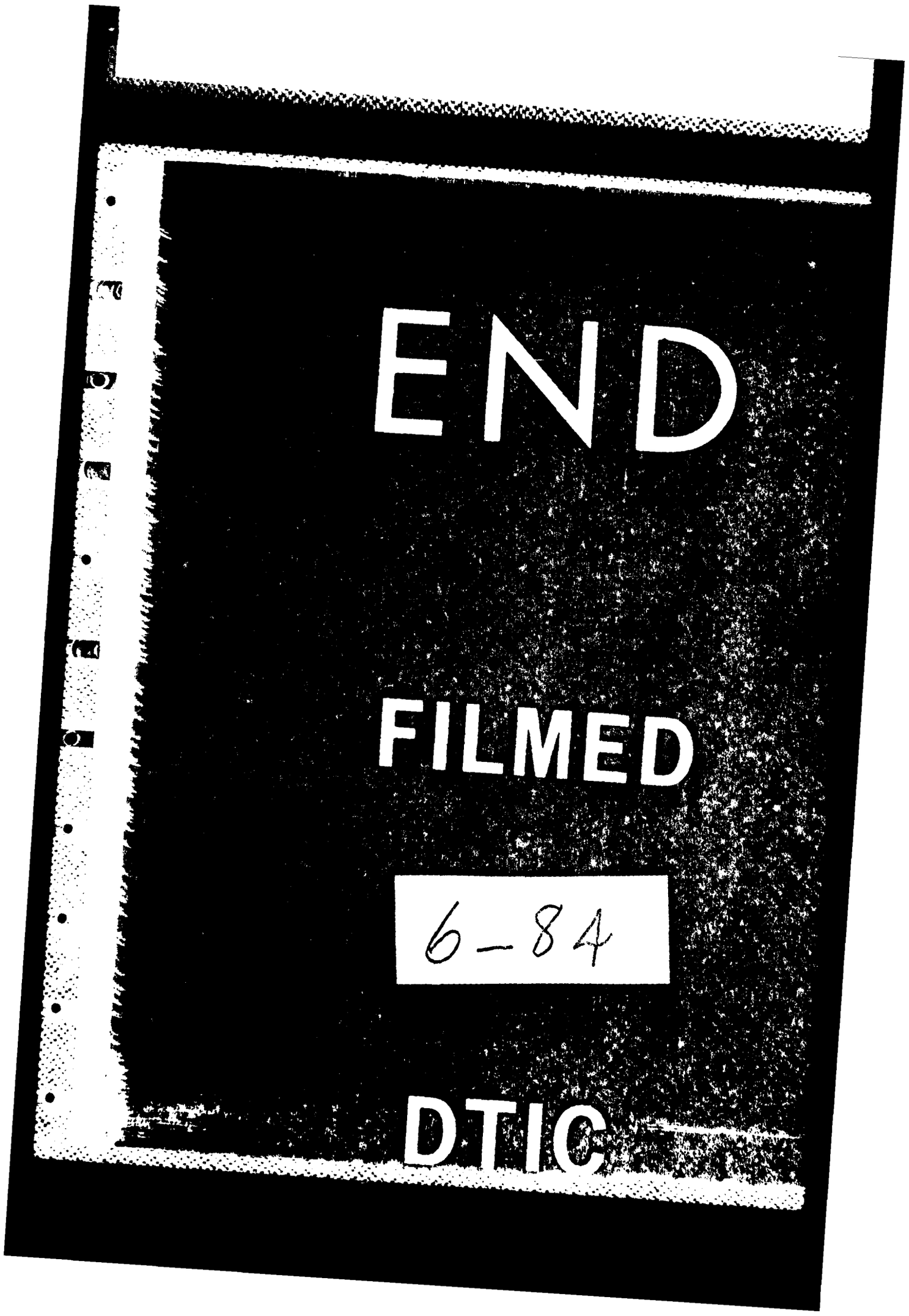
END
FILMED
6-84
DTIC